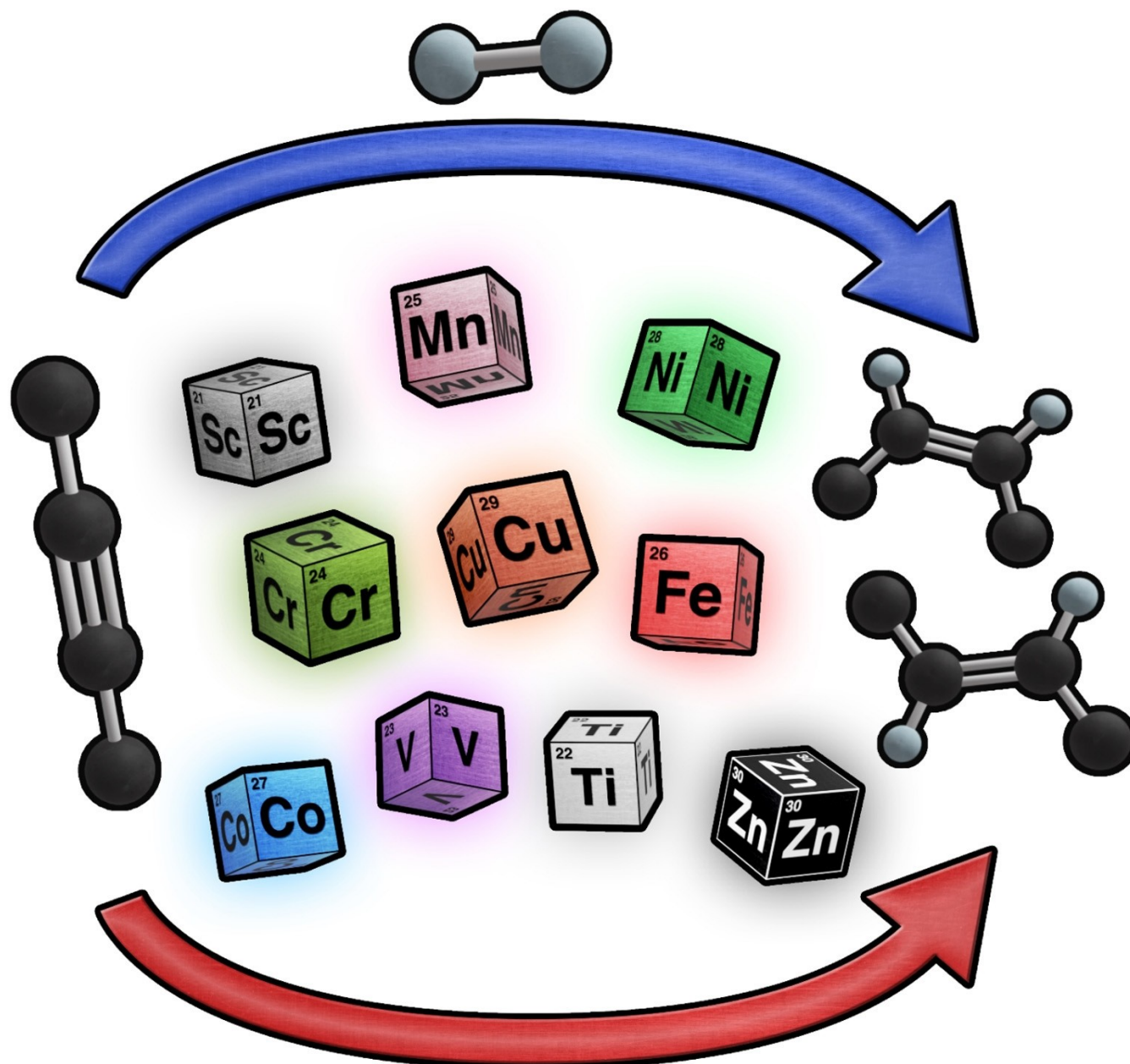


# Stereoselective Semi-Hydrogenations of Alkynes by First-Row (3d) Transition Metal Catalysts

Bernhard J. Gregori,<sup>[a]</sup> Mattis-Ole W. S. Schmotz,<sup>[a]</sup> and Axel Jacobi von Wangelin<sup>\*[a]</sup>

*Dedicated to Matthias Beller on the occasion of his 60<sup>th</sup> birthday*



The chemo- and stereoselective semi-hydrogenation of alkynes to alkenes is a fundamental transformation in synthetic chemistry, for which the use of precious 4d or 5d metal catalysts is well-established. In mankind's unwavering quest for sustainability, research focus has considerably veered towards the 3d metals. Given their high abundance and availability as

well as lower toxicity and noxiousness, they are undoubtedly attractive from both an economic and an environmental perspective. Herein, we wish to present noteworthy and groundbreaking examples for the use of 3d metal catalysts for diastereoselective alkyne semi-hydrogenation as we embark on a journey through the first-row transition metals.

## 1. Introduction

Reductive chemistry plays a pivotal role in the industrial preparation of numerous bulk chemicals. Hydrogenation reactions such as the Haber-Bosch process,<sup>[1]</sup> the hydrogenative saturation of fats<sup>[2]</sup> or the production of methanol fuel from CO or CO<sub>2</sub><sup>[3]</sup> are noteworthy examples, owing to their considerable impact on modern life. In general, the hydrogenation of alkenes or alkynes is of vital importance for the synthesis of myriad fine chemicals such as pharmaceuticals, fragrances and natural products (Scheme 1).<sup>[4,5,6]</sup> However, a partial hydrogenation of alkynes to alkenes remains a challenging task in catalysis for two main reasons: Firstly, the obtained alkenes may undergo facile onward hydrogenation to alkanes under similar catalytic conditions, which diminishes alkene yields and hampers product separation. High degrees of chemoselectivity between alkyne and alkene are crucial criteria for competent catalysts. While a plethora of active catalysts for the full hydrogenation of alkynes to alkanes have been developed, selective (3d) semi-hydrogenation catalysts have remained more limited. Secondly, a partial alkyne hydrogenation may produce two diastereomeric products: the (*E*)-alkene and the (*Z*)-alkene (occasionally referred to as *trans*- and *cis*-alkenes). Typically, only a single isomer is desired. Separation of *E/Z* product mixtures is notoriously problematic due to similar polarity and size, calling for high stereoselectivities in the catalytic step to avoid the undesired isomer altogether.

Ever since the pioneering works of Lindlar<sup>[7]</sup> for the *Z*-selective semi-hydrogenation of alkynes using a heterogeneous Pb-poisoned Pd catalyst, a multitude of potential catalytic systems has been developed,<sup>[8]</sup> a large portion of which are based on the later 4d or 5d transition metals. This is problematic from an economic as well as from an environmental perspective: The heavy 4d and 5d metals show a noticeably low abundance in the earth's crust and are difficult to mine and process, making them costly due to limited supply. Furthermore, due to their scarcity, they are foreign to most terrestrial organisms and thus generally show a high degree of toxicity

and potential environmental damage. An uprising field in green chemistry is to pursue new catalytic systems based on less toxic and environmentally benign elements such as 3d metals.<sup>[9]</sup> While few industrial processes are based on these metals, nature has been utilizing them for eons – indeed, most 3d metals can be found as an active center in metalloenzymes, proving their inherent potential as catalysts.<sup>[10]</sup> This review focuses on the diastereoselective semi-hydrogenation of alkynes to either the (*E*)- or (*Z*)-alkenes using H<sub>2</sub> gas and other hydrogen donors (transfer hydrogenations) and highlights current examples for 3d-metal-based catalysts. Herein, we provide an overview of the 3d elements starting with Sc, Ti, V and Cr, which have rarely been applied in semi-hydrogenation catalysis save a few examples, followed by Mn, often employed in transfer hydrogenation reactions. A large portion of this review is dedicated to Fe, Co, Ni and Cu as the most commonly utilized 3d metals in alkyne semi-hydrogenations, whereas Zn has thus far only been employed as an additive in the presence of another transition metal catalyst. The use of alternative methods of formal hydrogenations, *i.e.* via sequential hydrosilylation/hydroboration and protodesilylation/protodeboration is beyond the scope of this review. Topical reviews as well as most relevant recent works of such hydrofunctionalization methods will be referred to in the title of each chapter.

The main advantage of using molecular hydrogen (over alternative methods using boranes/silanes and protolytic work-up) is the avoidance of by-products and therefore the minimalization of waste. Common metrics of chemical sustainability are the atom economy, the environmental factor (E-factor), as well as hazard potentials, which all display beneficial magnitudes for the usage of H<sub>2</sub> gas as reductant.<sup>[9]</sup> Additionally, an economic cost-factor should be taken into consideration: While various silanes or boranes are rather inexpensive, the use of H<sub>2</sub> as the most widely available technical hydride source clearly should be preferred. Additionally, the growing production of “green hydrogen”, derived from large-scale electrolysis of water using exclusively renewable energies, paves the way for fully sustainable and climate-neutral protocols for both industrial as well as research applications.

[a] Dr. B. J. Gregori, M.-O. W. S. Schmotz, Prof. A. Jacobi von Wangelin  
Dept. of Chemistry, University of Hamburg  
Martin Luther King Pl 6  
20146 Hamburg (Germany)  
E-mail: axel.jacobi@uni-hamburg.de  
Homepage: <https://www.chemie.uni-hamburg.de/institute/ac/arbeitsgruppen/jacobi.html>

© 2022 The Authors. ChemCatChem published by Wiley-VCH GmbH. This is an open access article under the terms of the Creative Commons Attribution Non-Commercial NoDerivs License, which permits use and distribution in any medium, provided the original work is properly cited, the use is non-commercial and no modifications or adaptations are made.

## 2. Scandium<sup>[11,12]</sup>

As early transition metals are not intensively investigated as hydrogenation catalysts, only a single example for a selective semi-hydrogenation using dihydrogen was reported for scandium in 2017.<sup>[13]</sup> A scandium complex featuring a PNP-pincer ligand was applied as the catalyst for the hydrogenation of 3-hexyne under mild conditions (4 bar H<sub>2</sub>, 23 °C, 5 mol% catalyst).

The (*Z*)-alkene was obtained in high selectivity and yield (Scheme 2).

### 3. Titanium<sup>[11,14,15]</sup>

Similar to scandium, titanium-catalyzed (semi-)hydrogenation reactions have remained a rarity. The first report of a direct titanium-catalyzed semi-hydrogenation was published by Sonogashira and Hagihara in 1965.<sup>[16a]</sup> The authors employed  $[\text{Cp}_2\text{Ti}(\text{CO})_2]$  (Cp = cyclopentadienyl) as pre-catalyst in the semi-hydrogenation of just a handful of alkynes at 50 bar  $\text{H}_2$  and 50–60 °C after reaction in benzene or heptane for 30 min (Scheme 3a). 1-Pentyne, 1-hexyne and phenylacetylene were converted to the alkenes with yields of 95 %, 90 % and 95 %, respectively. However, *t*-butyl-acetylene afforded a 60/40 mixture of alkane and alkene; diphenylacetylene gave bibenzyl in 90 % yield; 3-heptyne showed no conversion. The authors speculated that a titanacyclopentadiene intermediate is operative, however, no mechanistic support was given. An optimized method was later reported by Dixneuf.<sup>[16b]</sup> Ligand substitution of the same pre-catalyst with trimethylphosphine in the presence of diphenylacetylene and subsequent treatment with  $\text{H}_2$  afforded the labile  $\text{Cp}_2\text{Ti}(\text{PMe}_3)$  complex that displayed very high activity and selectivity in the semi-hydrogenation of a few alkynes to the *Z*-alkenes. Full conversion was already observed at 1 bar  $\text{H}_2$  and room temperature (Scheme 3b).<sup>[16b]</sup>

Application of a ternary Pd@Cu/TiO<sub>2</sub> mixture as hydrogen transfer catalyst for alkyne reductions under ultraviolet light irradiation was reported in 2020.<sup>[17]</sup> The authors proposed a mechanism based on a photocatalytic cycle: The excitation of the photocatalyst (TiO<sub>2</sub>) in the UV generates an exciton. The positive holes are capable of oxidizing the hydrogen-donating isopropanol, producing acetone and protons. The electrons in the conduction band in combination with the protons subsequently form the active hydrogen species at the Pd@Cu-cocatalyst, which can selectively hydrogenate the alkyne to the (*Z*)-alkene.  $[\text{Cp}_2\text{Ti}^{\text{III}}\text{Cl}]$  was reported to act as a mediator in a

hydrogen transfer reaction from water.<sup>[18]</sup> A variety of well-known catalysts based on Pd, Rh or Ir were used as the actual hydrogenation catalyst, while the Ti(III) complex was employed in stoichiometric amounts for water reduction. One reported catalyst was the Lindlar catalyst, which afforded high *Z*-selectivities.

### 4. Vanadium<sup>[11,19]</sup>

Few systems are known for the semi-hydrogenation towards a single alkene isomer that directly involve vanadium. In 2011, a cationic vanadium complex was reported by Toste and co-workers which was capable of a highly selective conversion of alkynes under mild conditions (1 bar  $\text{H}_2$ , 60 °C, 24–72 h, 20 mol% [V]) to yield exclusively (*Z*)-alkenes.<sup>[20]</sup> Both internal and terminal alkynes were successfully converted using this method, however, only a small substrate scope of unfunctionalized substrates was presented, leaving the application of this method for functionalized substrates unclear. The authors provided a mechanistic proposal, involving a homogeneous bifunctional bis(imido)vanadium species (Scheme 4), which is capable of taking up one hydrogen molecule with contemporaneous formation of a monohydrido vanadium complex with one newly formed amido ligand. *Cis*-Hydrovanadation of the alkyne, followed by a 1,2- $\alpha$ -NH elimination with the amido ligand,<sup>[21]</sup> leads to liberation of the (*Z*)-alkene. Association of trimethylphosphine regenerates the initial catalyst species. This mechanistic proposal is based on DFT calculations, experiments with  $\text{H}_2/\text{D}_2$ -mixtures and parahydrogen-induced polarization (PHIP) NMR experiments. No scrambled HD-hydrogenation products have been observed and the PHIP-NMR experiment led to transfer of polarization; both of these results demonstrated that only one  $\text{H}_2$  molecule is involved in the hydrogenation of one alkyne molecule.

Two similar *Z*-selective vanadium-catalyzed hydrogenations of alkynes were reported in 2014<sup>[22]</sup> and 2017.<sup>[22]</sup> Both systems are based on organovanadium sites  $\text{V}(\text{Mes})(\text{thf})$  on either a



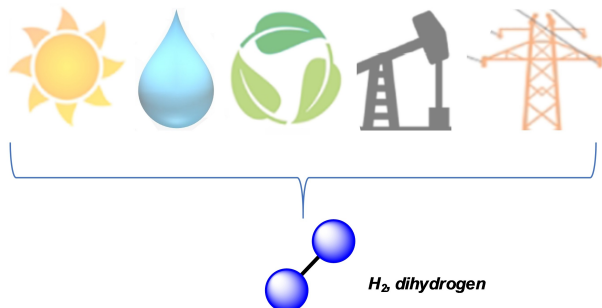
Bernhard J. Gregori hails from the picturesque banks of the Bavarian Danube. He studied Chemistry in Regensburg and graduated with a M.Sc. thesis on Fe-catalyzed hydrogenations. He continued his work on catalytic reductions at the University of Hamburg and was minted Dr. rer. nat. in 2021. Bernhard recently joined Alex Breder's team at the University of Regensburg.



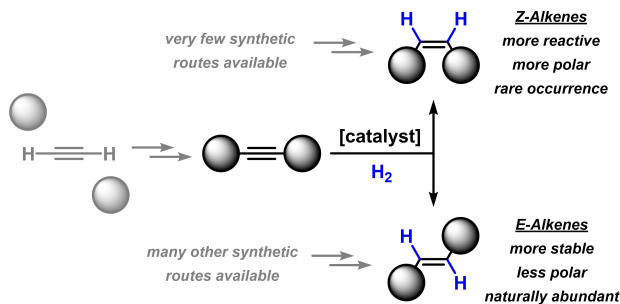
Mattis-Ole W. S. Schmotz is a native Hamburg kid. As an enthusiastic student at the University of Hamburg, he won the Best B.Sc. Student Prize and was awarded a fellowship of the fast track Ph.D. program of the Hamburg Research Academy. Mattis is engaged with research on photochemistry and catalysis.



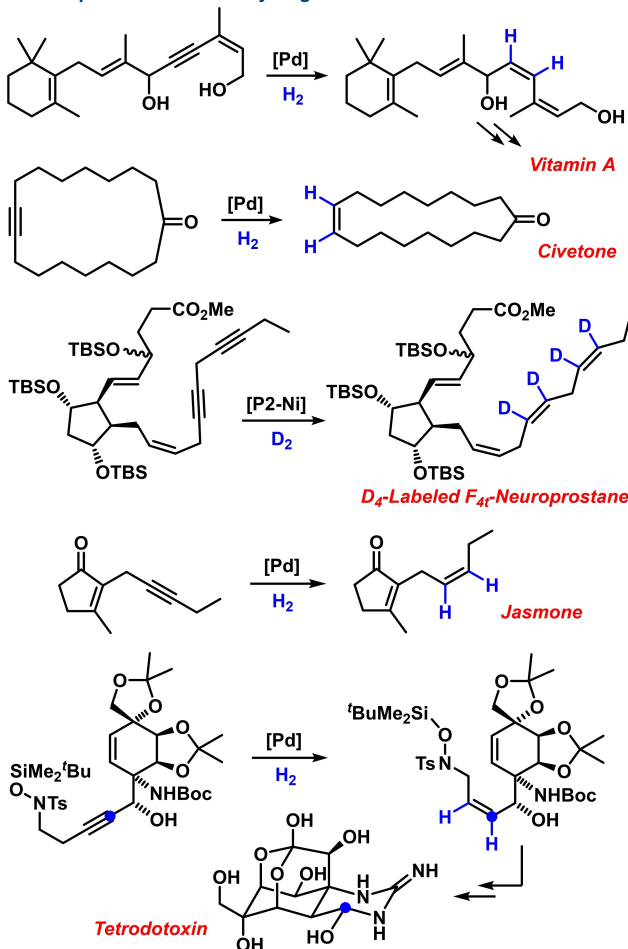
Axel Jacobi von Wangelin was born in Berlin and saw the graffiti-free side of the wall collapsing. He later enjoyed vibrant college lives in Erlangen, Utah, Cardiff, Rostock, Stanford, Cologne, and Regensburg. Axel is currently Professor of Molecular Chemistry at the University of Hamburg. His group's research spans all aspects of catalysis with special emphasis on earth-abundant metals and light-driven reactions.

— Wide availability of H<sub>2</sub> gas —

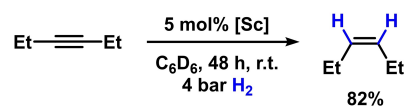
## — Stereoselective hydrogenation of alkynes —



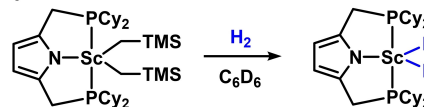
## — Examples of Z-selective hydrogenations —



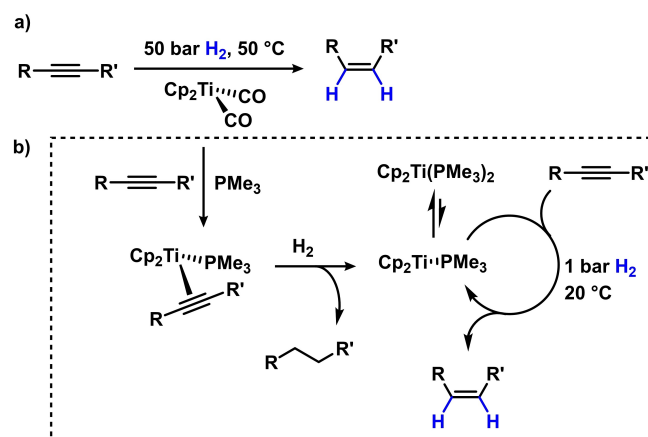
**Scheme 1.** Dihydrogen as a sustainable reductant and applications of selective semi-hydrogenations of alkynes in complex molecule syntheses.<sup>[4,5]</sup>



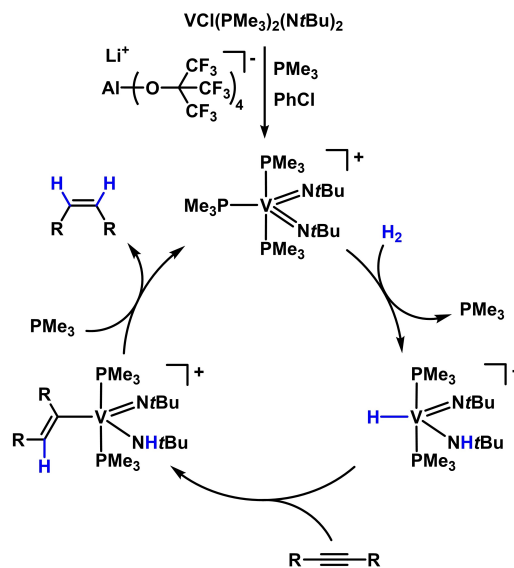
pre-catalyst:



**Scheme 2.** Application of a PNP-scandium complex for Z-selective semi-hydrogenation of an internal alkyne. A dihydrido complex was proposed as active species.<sup>[13]</sup>

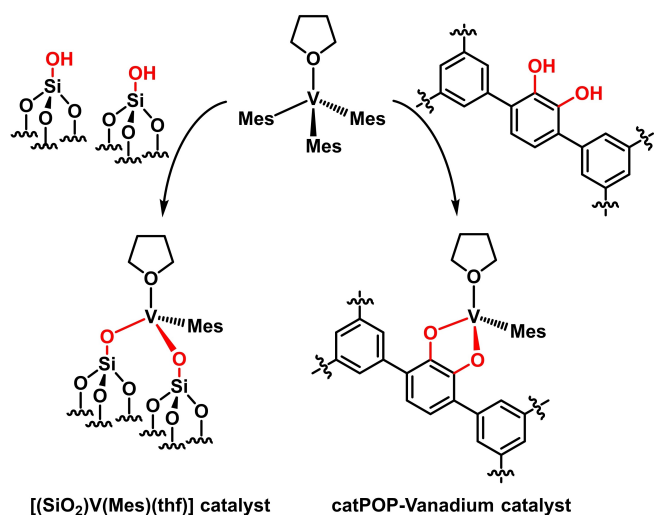


**Scheme 3.** a) Ti-catalyzed semi-hydrogenations by Sonogashira;<sup>[16a]</sup> and b) optimized conditions for low-pressure hydrogenations by Dixneuf.<sup>[16b]</sup>



**Scheme 4.** Preparation of the cationic vanadium catalyst and proposed mechanism for the selective semi-hydrogenation.<sup>[19]</sup>

catechol-functionalized porous organic polymer (catPOP)<sup>[22]</sup> or on silica, SiO<sub>2</sub> (Scheme 5).<sup>[23]</sup> Both catalysts exhibit a similar structural motif. The former authors<sup>[22]</sup> reported 37% conversion

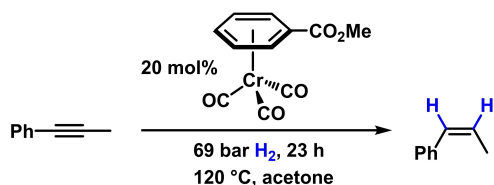


**Scheme 5.** Structural motifs of the  $[(\text{SiO}_2)\text{V}(\text{Mes})(\text{thf})]$ - as well as the catPOP-vanadium catalyst. Structure proposals based on XAS and EPR.<sup>[22,23]</sup>

of diphenyl-acetylene with exclusive formation of stilbene (*Z/E* 98/2, 1.2 mol%  $[(\text{catPOP})\text{V}(\text{Mes})(\text{thf})]$ , 14 bar  $\text{H}_2$ , 60 °C, 8 h, methylcyclohexane). Full conversion is observed with higher catalyst loading, albeit accompanied by increasingly significant amounts of over-hydrogenation products. The latter authors<sup>[23]</sup> reported 88–91% conversion of diphenylacetylene with 78–90% formation of stilbene (*Z/E* not given, 0.4–0.5 mol%  $[(\text{SiO}_2)\text{V}(\text{Mes})(\text{thf})]$  with different  $\text{SiO}_2/\text{V}$  ratios, 14 bar  $\text{H}_2$ , 75 °C, 1–17 h, dodecane). Upon longer reaction times, the catalyst led to the further conversion of the alkene to the fully hydrogenated alkane.

## 5. Chromium<sup>[11]</sup>

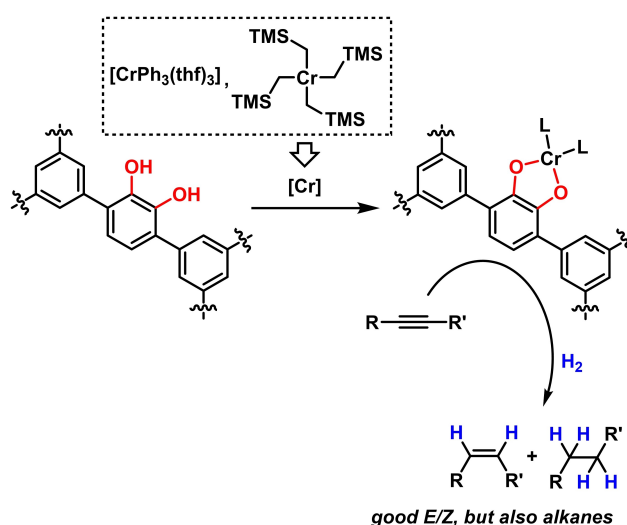
The earliest report on chromium-catalyzed selective semi-hydrogenation of alkynes stems from Sodeoka and co-workers, published in 1985.<sup>[24]</sup> They demonstrated the application of “piano stool” (arene)tricarbonylchromium(0) complexes as highly efficient catalysts (Scheme 6). 1-Phenyl-1-propyne was successfully hydrogenated (20 mol%  $[\text{Cr}]$ , 69 bar  $\text{H}_2$ , 120 °C, acetone) to (*Z*)-1-phenyl-1-propene in high yield, while no (*E*)-isomer or fully hydrogenated alkane have been observed, even under prolonged reaction times. However, a limited substrate scope was reported and the harsh conditions left room for an improvement of this protocol. Akin to the catPOP-vanadium



**Scheme 6.** *Z*-Selective semi-hydrogenation of 1-phenyl-1-propyne using a (methyl benzoate)tricarbonylchromium(0) complex.<sup>[24]</sup>

system (vide supra), a similar chromium-based system has been developed (Scheme 7). The initial report relied on  $[\text{Cr}(\text{CH}_2\text{SiMe}_3)_4]$  as the precursor,<sup>[22]</sup> which was later substituted by  $[\text{CrPh}_3(\text{thf})_3]$ <sup>[25]</sup> due to improved protonolysis behavior and increased stability towards decomposition. These effects led to a more defined catalytic system, which was formed within 2 h instead of the prolonged reaction times or elevated temperatures otherwise necessary. Both catalytic systems show high efficiency towards (semi-)hydrogenation, with the earlier report exhibiting a higher activity towards full hydrogenation of diphenylacetylene (81% 1,2-diphenylethane, 19% (*Z*)-stilbene) than the  $[\text{CrPh}_3(\text{thf})_3]$ -based catalyst, which predominantly resulted in the formation of (*Z*)-stilbene (35% (*Z*)-stilbene, 1% (*E*)-stilbene, 6% 1,2-diphenylethane) under the same conditions (5 mol%  $[\text{Cr}]$ , 14 bar  $\text{H}_2$ , 60 °C, 6 h, methylcyclohexane). As a mechanistic proposal for the observed activity and the function of the catecholate moiety, the authors suggested that, upon dissociation of a THF molecule, a free coordination site for the alkyne is provided on the Cr center. Additionally, free coordination sites for hydrogen are required. The polymeric catecholate ligand inhibits the formation of chromium dimers and consequent loss of catalytic activity due to the blockage of coordination sites. The authors verified this proposal by poisoning the active catalyst with bipyridine, resulting in a total loss of hydrogenation activity.

A recent development in Cr-catalyzed semi-hydrogenation was the application of commercially available  $[\text{Cr}(\text{acac})_3]$  in combination with the reductant diisobutylaluminium hydride (DIBAL-H) in THF.<sup>[26]</sup> While  $\text{CrCl}_2$  and  $\text{CrCl}_3$  (entries 1 and 2, table 1), showed low conversions towards the alkene,  $\text{Cr}(\text{acac})_3$  provided an efficient and simple catalytic process for the selective semi-hydrogenation under mild conditions (5–10 mol% catalyst, < 5 bar  $\text{H}_2$ , 25 °C, 3–24 h, THF). A variety of functional groups such as halides, ethers, esters, and ketones were tolerated under these conditions. The highest selectivity towards (*Z*)-alkenes was achieved with dialkylacetylenes, com-



**Scheme 7.** Precursors for the preparation of catPOP-chromium catalysts. Structures were proposed based on XAS and EPR.<sup>[22][25]</sup>

**Table 1.** Chromium-catalyzed semi-hydrogenation of alkynes.<sup>[26]</sup>

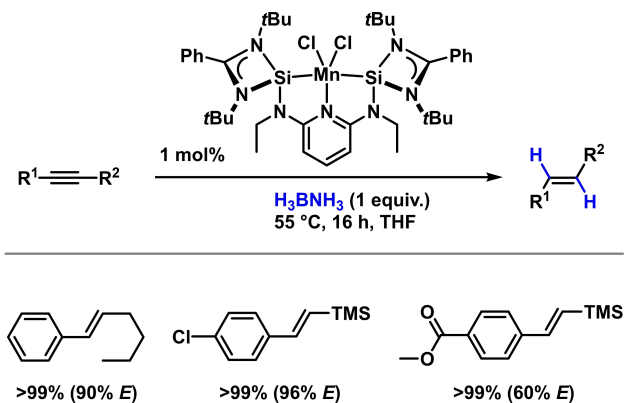
Entry	Alkyne	Alkene [%] <sup>[a]</sup>	Z/E <sup>[a]</sup>
1 <sup>[b]</sup>		19	17/1
2 <sup>[c]</sup>		28	16/1
3 <sup>[d]</sup>		51	12/1
4 <sup>[e]</sup>		95	6/1
5 <sup>[f]</sup>		96	3/1
6 <sup>[g]</sup>		97	10/1
7		99	> 99/1

Conditions: 0.2 mmol alkyne, 0.4 mL THF. [a] Determined by <sup>1</sup>H-NMR, GC-FID. [b] 5 mol% CrCl<sub>2</sub>, 10 mol% DIBAL-H. [c] 5 mol% CrCl<sub>3</sub>, 15 mol% DIBAL-H. [d] 5 mol% [Cr(acac)<sub>3</sub>], 15 mol% DIBAL-H. [e] 1.3 bar H<sub>2</sub>, 9 h. [f] 3 bar H<sub>2</sub>. [g] 12 h.

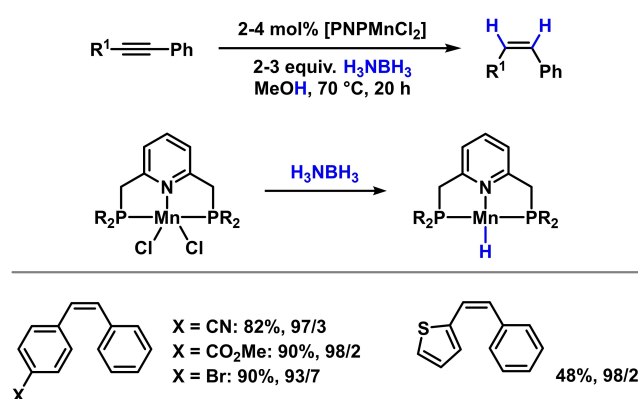
pared to the lower selectivity for diarylacetylenes. Mechanistically, the acetylacetonate is initially reduced; this has been confirmed by the isolation of the reduced species (removal of carbonyl group, reduction to alcohols with subsequent elimination to alkene products). Additionally, the chromium is reduced, which results in an aggregation to Cr nanoparticles, which have been detected by TEM.

## 6. Manganese<sup>[11,27–30]</sup>

While various examples for full hydrogenations using manganese catalysts are known, the semi-hydrogenation of alkynes remains a challenging task.<sup>[31]</sup> The first reports were contemporaneously published by Zhou et al.<sup>[32]</sup> and Brzowska et al.<sup>[33]</sup> in 2018. Both systems rely on hydrogen donors to carry out a transfer semi-hydrogenation. Zhou and co-workers applied an *N*-heterocyclic silylene manganese complex (1 mol%) in THF at 55 °C for the *E*-selective transfer hydrogenation of alkynes, using ammonia borane as the hydrogen source (Scheme 8).<sup>[32]</sup> A variety of functional groups such as ethers, halides, or esters were tolerated and gave the semi-hydrogenation product with high yield and *E*-selectivity. Mechanistic proposals for the observed reactivity are based on the formation of a molecular Mn-hydrido complex by means of the ammonia borane. No conversion under H<sub>2</sub> atmosphere was observed in the absence of H<sub>3</sub>N-BH<sub>3</sub>. Unfortunately, no proposals for the origin of the *E*-selectivity were provided. Similarly, the system by Brzowska et al.<sup>[33]</sup> utilized a PNP-pincer ligand and ammonia borane in methanol as the hydrogen donor for the *Z*-selective semi-hydrogenation of alkynes in generally high yields (see Scheme 9). Analogously to the system of Zhou et al., it was hypothesized that the initial alkoxido-Mn complex undergoes ligand substitution to a hydrido complex by means of ammonia borane. Subsequent *cis*-hydrometallation and protonation of the intermediate vinyl complex by methanol regenerates the

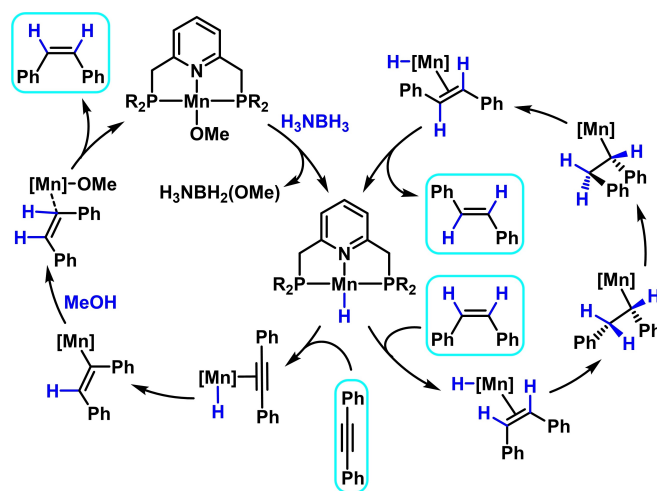


**Scheme 8.** Silylene-manganese catalyst for *E*-selective semi-hydrogenation. Conversions are given; *E*-selectivity in parentheses.<sup>[32]</sup>



**Scheme 9.** A PNP-pincer manganese complex for the *Z*-selective semi-hydrogenation of alkynes applied to various substrates.<sup>[33]</sup> Isolated yields and *Z/E* ratios are given next to each substrate.

alkoxido species and releases the (*Z*)-alkene (Scheme 10). The presence of small amounts of (*E*)-alkene was explained by



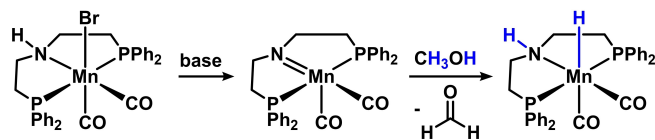
**Scheme 10.** Proposed mechanism of PNP/manganese-catalyzed hydrogenation (left) and isomerization (right); from DFT calculations; R = 'Pr.<sup>[33]</sup>

isomerization in a second catalytic cycle. However, the coordination of the alkyne to the Mn center is energetically preferred over the (*Z*)-alkene coordination and thus the isomerization is limited.

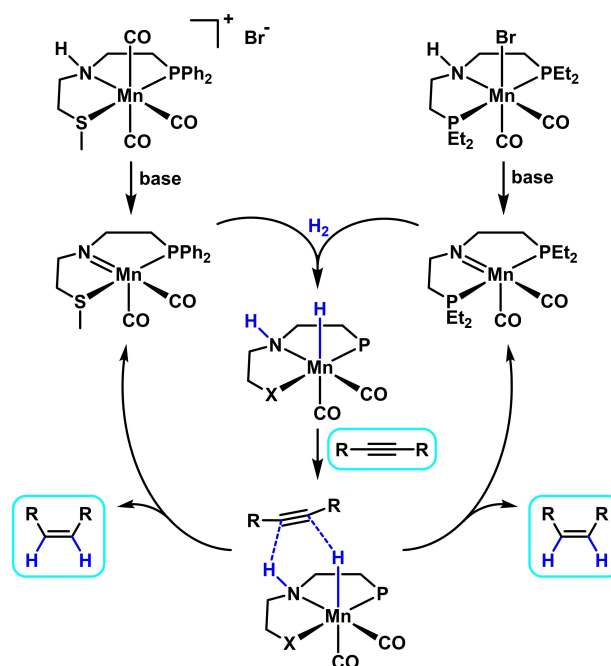
The same group later reported a similar catalyst based on a [MnBr(CO)<sub>2</sub>(PNP)] for *Z*-selective semi-hydrogenation without relying on ammonia borane as a hydride donor; both hydrogen atoms stem from methanol (Scheme 11).<sup>[34]</sup> After elimination of HBr by means of a base, methanol protonates the Mn=N bond and coordinates to the Mn center, resulting in a manganese methoxide intermediate.  $\beta$ -Hydride elimination releases formaldehyde and generates a hydrido species, which further reacts with the alkyne under standard hydrometallation-protonation steps to form the (*Z*)-alkene. The system operates under forcing conditions: 150 °C, 2 equivalents of Cs<sub>2</sub>CO<sub>3</sub> as the base and 14 h of reaction time in a methanol/toluene mixture are required. Nonetheless, the authors report a broad substrate scope with high yields and *Z*-selectivities.

In a recent example, Torres-Calis and García reported an *E*-selective semi-hydrogenation of internal alkynes using isopropanol as the sole hydrogen source and [MnBr(CO)<sub>3</sub>(dippe)] as pre-catalyst (dippe = 1,2-bis(diisopropylphosphino)ethane) under basic conditions (4 mol% [Mn], 10 mol% NaOMe, <sup>*i*</sup>PrOH/THF, 100 °C, 4 h).<sup>[35]</sup> The authors proposed an initial displacement of the bromido by isopropanolate, followed by  $\beta$ -hydride elimination to provide a hydridomanganese complex. Subsequent hydrometallation of the alkyne and proto-demetalation by isopropanol gave the (*Z*)-alkene. In a separate cycle, the (*Z*)-alkene is isomerized, dictated by the thermodynamic equilibrium between *E*- and *Z*-isomers. Diphenyl acetylene was converted to stilbene with 98% yield and *E/Z* = 97/3. Substituted diarylalkynes generally gave much lower yields and selectivities; 4-(phenylethynyl)toluene afforded the alkene in 51% yield with *E/Z* = 52/48. Dialkylalkynes were unreactive.

The first two examples for a direct semi-hydrogenation using gaseous H<sub>2</sub> as opposed to a transfer hydrogenation were reported nearly parallel by Zubar et al.<sup>[36]</sup> and by Garbe et al.<sup>[37]</sup> Both systems again operated with pincer-manganese complexes, which form the active hydride species upon hydrogenation of the Mn=N double bond in the presence of a base. It was proposed<sup>[36,37,38]</sup> that the alkyne hydrogenation step occurs via an outer-sphere mechanism (Scheme 12). Similar reaction conditions were applied in both cases, employing 1–5 mol% [Mn], 2.5 equiv. KO<sup>*t*</sup>Bu with respect to [Mn], 30–60 °C, 20–30 bar H<sub>2</sub> and 16 h in a non-polar solvent (heptane or toluene). High



**Scheme 11.** A PNP-manganese complex for the semi-hydrogenation using methanol as the hydrogen source. Both the hydrido ligand on manganese as well as the hydrogen atom on the nitrogen were proven to originate from methanol.<sup>[34]</sup>



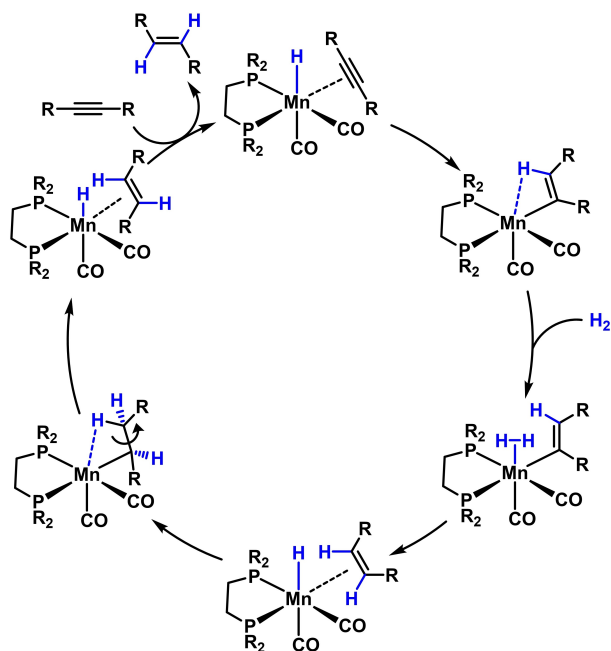
**Scheme 12.** Comparison between two Mn catalysts for the semi-hydrogenation of alkynes using H<sub>2</sub>. After initial formation of the hydrido-Mn species, an outer sphere mechanism was proposed for the alkyne hydrogenation step.<sup>[35,36,37]</sup> Top left: Mn catalyst of Zubar et al.<sup>[36]</sup> Top right: Mn catalyst of Garbe et al.<sup>[37]</sup> P and X are used as placeholders.

yields (> 90%) and high selectivities (> 90/10) towards the (*Z*)-alkenes were achieved.

A recent example of an *E*-selective semi-hydrogenation was reported by Farrar-Tobar and co-workers employing a Mn hydrido complex as the catalytically active species.<sup>[39]</sup> The reaction proceeds both with gaseous H<sub>2</sub> (1 mol% [Mn], 30 bar H<sub>2</sub>, 16 h, 60 °C, toluene) and H<sub>2</sub> generated *in situ* from the methanolysis of KBH<sub>4</sub> (1 mol% [Mn], 0.5 equiv. KBH<sub>4</sub>, 20 h, 90 °C, MeOH). The authors performed mechanistic experiments and detailed DFT calculations that suggest a *Z*-selective hydrogenation step, followed by an isomerization to the (*E*)-alkene (Scheme 13). This protocol tolerated esters, aryl halides (F, Cl, Br), alcohols and phenols, amines and heteroarenes. The use of *in situ* generated hydrogen instead of 30 bar H<sub>2</sub> drastically improved the yields and selectivities of the reaction (Table 2). Dialkyl-substituted alkynes showed high yields of alkene, but only low selectivities of 67–75% for the *in situ* method.

## 7. Iron<sup>[11,27,40,41]</sup>

Some of the earliest reports for iron-catalyzed semi-hydrogenations of alkynes stem from Thompson and co-workers as far back as the 1940s<sup>[42]</sup> and from Y. Urushibara, eponymous for the Urushibara catalyst, in the 1960s.<sup>[43]</sup> Thompson used an iron-aluminium alloy, however, only very few aliphatic alkynes were successfully hydrogenated to (*Z*)-alkenes at 70–100 bar H<sub>2</sub> and 100–150 °C.<sup>[42]</sup> A similar Fe–Al alloy catalyst was later described by Armbrüster et al.<sup>[44]</sup>



**Scheme 13.** Mechanistic proposal for the Z-selective semi-hydrogenation catalyzed by an Mn-H complex.<sup>[39]</sup> R = <sup>i</sup>Pr.

**Table 2.** Use of an alkyl-Mn pre-catalyst for the E-selective hydrogenation of internal alkynes using two different H sources.<sup>[39]</sup>

Alkyne	Conditions A		Conditions B	
	Alkyne	E/Z [%]	Alkyne	E/Z [%]
	> 99	> 99/1	> 99	> 99/1
	90	> 99/1	96	> 99/1
	99	> 99/1	44	98/2
	69 <sup>[a]</sup>	> 99/1	traces	/
	95	99/1	75	> 99/1
	99 <sup>[b]</sup>	98/2	54	73/27
	99	67/33	91	80/20

[a] 25 h, [b] 2 mol% [Mn].

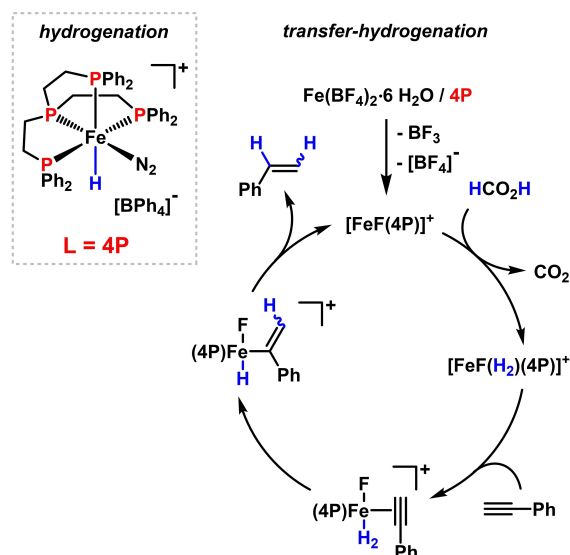
The Urushibara catalyst<sup>[43]</sup> is prepared by reducing an iron precursor (hydrates of FeCl<sub>2</sub> or FeCl<sub>3</sub>) with zinc dust in water. After the exothermic reaction has ceased, the heterogeneous catalyst is washed with water and digested with acetic acid to obtain a powder which was subsequently applied as a catalyst for the Z-selective hydrogenation of alkynes (2-butyne-1,4-diol). However, high catalyst loadings (>50 wt%, due to a low catalyst surface area), and temperatures (80–100 °C, due to hydrogen uptake only starting at 80 °C) as well as an elevated H<sub>2</sub> pressure (> 50 bar) were required. With these harsh reaction

conditions, alternative iron-catalyzed processes were highly desirable.

The [CpFe(μ<sub>3</sub>-CO)]<sub>4</sub> cluster has been employed for the semi-hydrogenation of terminal and internal alkynes at elevated pressure (7–70 bar H<sub>2</sub>) and temperatures (100–140 °C) by Pittman and co-workers.<sup>[45]</sup> Internal alkynes reacted more sluggishly compared to terminal alkynes, the latter of which underwent slow isomerization to internal alkenes if alkyl-substituted. No full hydrogenation to alkanes was observed.

Bianchini et al.<sup>[46]</sup> reported a semi-hydrogenation of terminal alkynes using the PPPP-pincer-Fe hydride complex ([FeH(P(CH<sub>2</sub>CH<sub>2</sub>PPh<sub>2</sub>)<sub>3</sub>)(X<sub>2</sub>)]BPh<sub>4</sub>, X = H, N). Terminal alkynes were hydrogenated at 1 bar H<sub>2</sub> and 20–60 °C (Scheme 14).

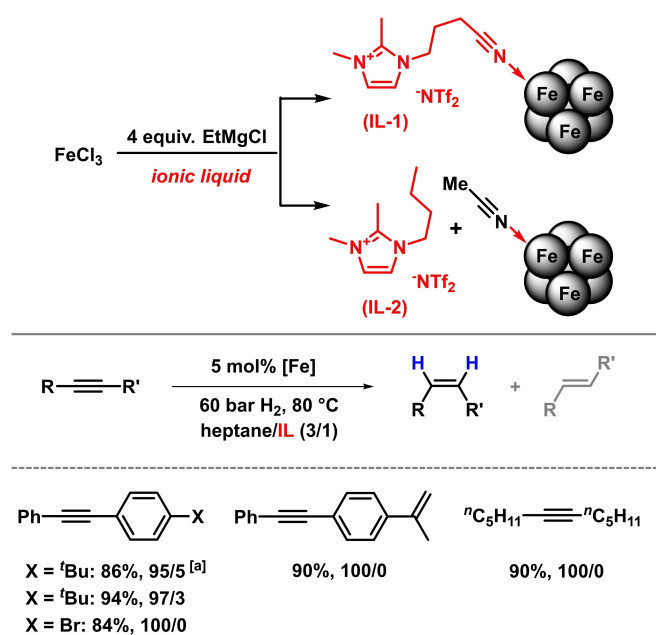
A similar catalyst was applied to the transfer hydrogenation of terminal alkynes by Wienhöfer et al. in 2012.<sup>[47]</sup> Fe(BF<sub>4</sub>)<sub>2</sub>·6 H<sub>2</sub>O was employed in the presence of the tetraphos ligand (P(CH<sub>2</sub>CH<sub>2</sub>PPh<sub>2</sub>)<sub>3</sub>) with formic acid acting as the hydrogen donor (Scheme 14). Under optimized conditions (0.75–2.5 mol% [Fe], 2–3 equiv. formic acid, 40 °C, 5 h, THF), numerous terminal alkynes were converted quantitatively to alkenes while no full hydrogenation to alkanes was observed. Functional groups such as halides, esters, or alcohols were well tolerated. An iron hydride similar to the Bianchini complex<sup>[46]</sup> was proposed to form by decarboxylation of the intermediate formate complex. After coordination of the alkyne, the two H atoms are successively added to the alkyne by means of hydrometallation and reductive elimination. Deuteration experiments using DCO<sub>2</sub>H for the hydrogenation of 4-acetylphenylacetylene showed ~50% deuteration of the α-position of the styrene, verifying the presence of an initial [Fe(HD)] species. Moreover, the β-position is non-selectively deuterated to yield a 1:1 E/Z-mixture.



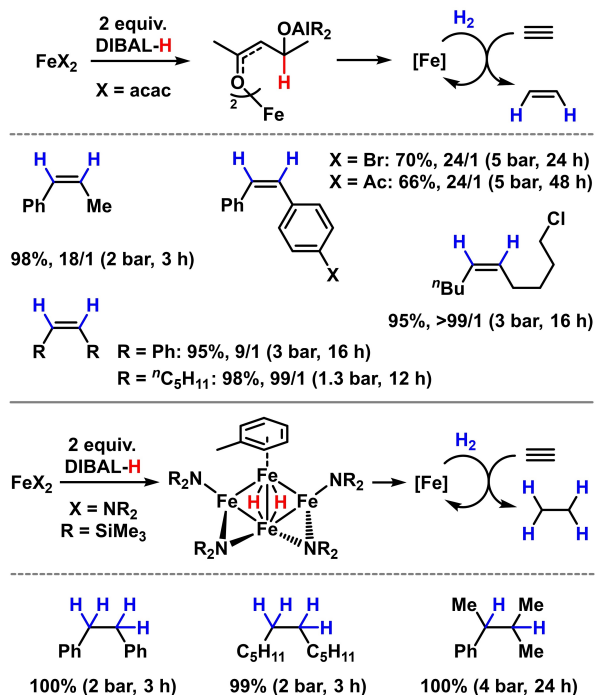
**Scheme 14.** Left: Fe-tetraphos-catalyst of the semi-hydrogenation of terminal alkynes by Bianchini et al.<sup>[46]</sup> Right: Related transfer-hydrogenation mechanism by Wienhöfer et al. using formic acid (4P = tetraphos = (P(CH<sub>2</sub>CH<sub>2</sub>PPh<sub>2</sub>)<sub>3</sub>)).<sup>[47]</sup>



The iron catalysts of Bart et al.<sup>[48]</sup> and Gieshoff et al.,<sup>[49]</sup> albeit developed for full hydrogenation to alkanes, initially form *Z*-



**Scheme 15.** An Fe-nanoparticle-catalyzed semi-hydrogenation of alkynes in a biphasic organic solvent/ionic liquid medium.<sup>[50]</sup> Reaction conditions with IL-2: 5 mol% [Fe], 1 equiv. MeCN, 60 bar H<sub>2</sub>, 80 °C, 18 h, heptane/[BMMIm]NTf<sub>2</sub> (3/1). Yields (GC, <sup>1</sup>H-NMR) and *Z/E* ratios are given below each substrate. [a] reaction in IL-1, reaction time 48 h.



**Scheme 16.** Iron-catalyzed *Z*-selective semi-hydrogenation of alkynes under mild conditions (top). Role of the anionic ligand on the chemoselectivity of the catalyst (X = acac vs. N(SiMe<sub>3</sub>)<sub>2</sub>).<sup>[51,52]</sup>

alkenes by semi-hydrogenation of several internal alkynes, which can be obtained at shorter reaction times.

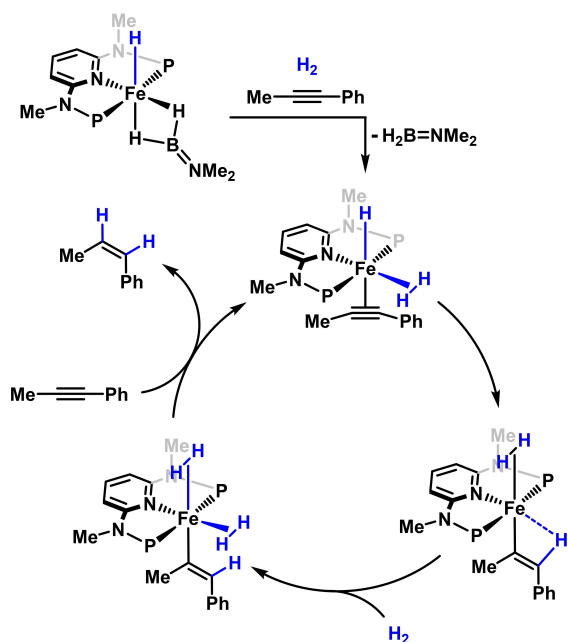
Another interesting approach was presented by the latter group already in 2014, which relied on a biphasic solvent/ionic liquids system containing iron nanoparticles, generated *in situ* by reduction of FeCl<sub>3</sub> with ethylmagnesium chloride (Scheme 15).<sup>[50]</sup> *Z*-Selective semi-hydrogenation was accomplished by attaching a nitrile moiety to the cation to serve as a selective catalyst poison to impede the otherwise occurring full hydrogenation, which is also observed in the absence of the ionic liquid altogether. Structural separation of the nitrile and ionic liquid functions by using a combination of acetonitrile and the commercially available ionic liquid [BMMIm]NTf<sub>2</sub> gave superior catalyst activities and stereoselectivities. The main advantage of this system lies in the fact that the ionic liquid may be reused several times (up to 8 reaction cycles) after phase separation, during which the IL-stabilized iron nanoparticles remain in the IL phase, whereas the hydrogenation products remain in the organic phase. Disadvantageously, harsh reaction conditions proved necessary for this biphasic system, due to the sluggish interphase hydrogen transfer and the high viscosity of the ionic liquid at lower temperatures. Thus, the same group opted for a method with milder reaction conditions.<sup>[51]</sup> The reaction of Fe(acac)<sub>2</sub> with DIBAL-H in THF yielded a heterotopic catalyst capable of *Z*-selective semi-hydrogenation of alkynes under very mild conditions (1–5 bar H<sub>2</sub>, 30 °C; Scheme 16). The observed reactivity may be explained by a “buffering” effect of the acetylacetonate ligand due to an initial ligand-centered reduction, followed by a delayed, intramolecular reduction of the iron center. This effect prevents an otherwise rapid total reduction of the Fe(II) species and consequent agglomeration to larger particles (observed with TEM). This study additionally investigated the reduction step via XANES and EXAFS spectroscopy and compared it to the reduction of Fe(hmnds)<sub>2</sub> (hmnds = 1,1,1,3,3,3-hexamethyldisilazane), the latter having been applied as an efficient catalyst for full hydrogenation to alkanes under comparable reaction conditions (Scheme 16).<sup>[52]</sup> The reduction of Fe(hmnds)<sub>2</sub> by DIBAL-H initially results in a cluster structure, which subsequently undergoes further agglomeration in the presence of additional reductant.

In 2017, Tejada-Serrano and co-workers reported a highly *Z*-selective semi-hydrogenation by means of iron(II,III) oxide nanoparticles immobilized onto an acidic metal oxide (ZnO, TiO<sub>2</sub>, ZrO<sub>2</sub>).<sup>[53]</sup> High conversions and selectivities were observed for most substrates at 10 bar H<sub>2</sub> and 100 °C. Additionally, this method offers a remarkable approach for the industrial removal of residual acetylene from a stream of ethylene gas, where the presence of alkynes may pose a problem for subsequent catalytic conversions of the alkene (e.g. polymerization). It was hypothesized that surface hydroxyl groups on the metal oxide solid support assist in the dissociation of coordinated hydrogen.

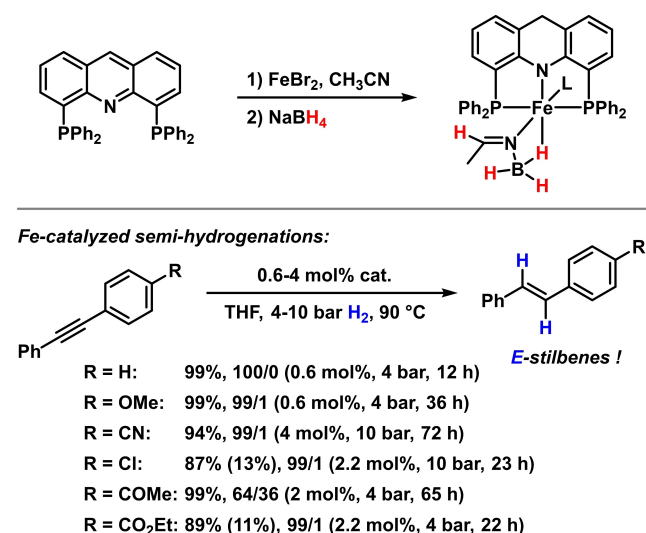
In 2019, Gorgas et al.<sup>[54]</sup> reported a *Z*-selective semi-hydrogenation using a bench-stable cationic hydridoiron(II) complex, featuring a PNP-pincer as well as an aminoborane ligand. The active hydrido-dihydrogen complex is generated upon addition of hydrogen. Whilst terminal alkynes showed complete hydro-

genation to the corresponding alkanes, this method delivered exclusively (*Z*)-alkenes when internal alkynes, 1,3-diynes, or 1,3-enynes were hydrogenated, whereas no (*E*)-alkenes or alkanes were observed at 5 bar H<sub>2</sub> after 1 h at room temperature. DFT calculations were performed to provide mechanistic insights (Scheme 17).<sup>[54]</sup>

Beside these examples for a *Z*-selective semi-hydrogenation, a handful of protocols have been reported for *E*-selective hydrogenations by means of iron catalysis. The first report by Srimani and co-workers<sup>[55]</sup> used a PNP-pincer-Fe complex for an



**Scheme 17.** PNP-Fe-complex-catalyzed semi-hydrogenation of internal alkynes. (P = PPr<sub>2</sub>, positive charges of the Fe complexes omitted for clarity).<sup>[54]</sup>



**Scheme 18.** A PNP-iron complex for the *E*-selective semi-hydrogenation of internal alkynes. GC yields of alkene, GC yields of alkane (in parentheses, if applicable), *E/Z* ratios, and reaction conditions are given next to each substrate.<sup>[55]</sup>

*E*-selective semi-hydrogenation at 90 °C and low hydrogen pressure (Scheme 18). Various functionalized alkynes were converted with high yield and selectivity. For some substrates, the fully hydrogenated alkane products could be observed, necessitating defined reaction conditions for every substrate by variation of reaction time and pressure. Isomerization experiments with (*Z*)-stilbene verified the *E*-selectivity of the overall reaction: After initial *Z*-selective semi-hydrogenation, the (*Z*)-alkene undergoes rapid isomerization to its (*E*)-isomer. A bimetallic catalyst for *E*-selective semi-hydrogenation was reported by Karunananda and Mankad.<sup>[56]</sup> Whereas iron could be included as part of the catalyst, the study mainly focused on ruthenium due to higher conversion and improved selectivity. The mechanistic proposal, based on DFT calculations of the transition state, implies that the hydrogenation step operates *Z*-selectively at the "second" metal (copper or silver) and iron or ruthenium are responsible for the hydrogen activation.<sup>[56]</sup> A subsequent isomerization step leads to the formation of the (*E*)-alkene. In 2019, Espinal-Viguri and co-workers reported a (nacnac)Fe-catalyzed *E*-selective transfer-hydrogenation using a borane as the hydride source and an amine as the proton source.<sup>[57]</sup> This method was mainly applied for the hydrogenation of alkenes, however, a single internal and a handful of terminal alkynes were converted to the corresponding alkenes when one equivalent of amine and borane each is employed.

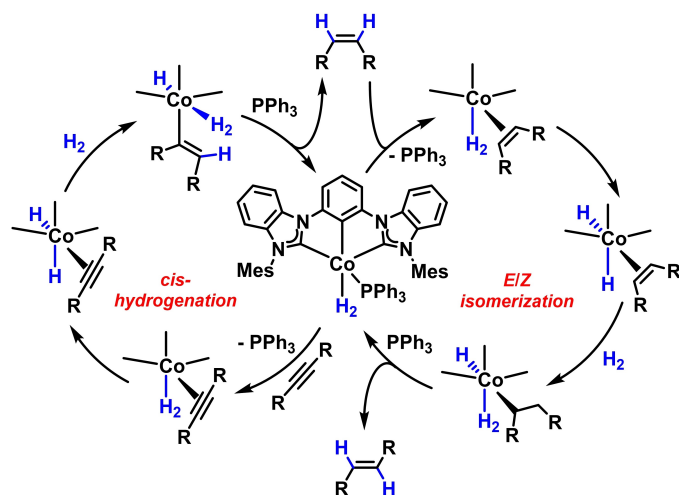
In addition to the methods presented here, a multitude of different systems have been reported for which a semi-hydrogenation of alkynes could be observed upon shorter reaction times, although the intermediate alkenes were generally further hydrogenated as the reaction progressed.<sup>[58]</sup>

## 8. Cobalt<sup>[11,27,59,60]</sup>

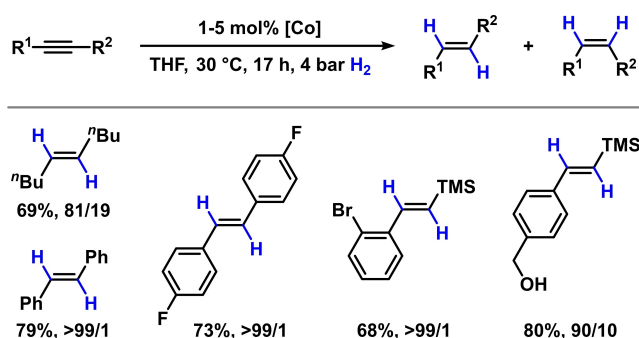
An early example of cobalt-catalyzed semi-hydrogenation utilized the hydridocobalt complexes ([CoH(CO)<sub>2</sub>(P<sup>n</sup>Bu<sub>3</sub>)<sub>2</sub>]) and [CoH(CO)(P<sup>n</sup>Bu<sub>3</sub>)<sub>3</sub>].<sup>[61]</sup> Both catalysts enabled selective hydrogenations of 1-pentyne to 1-pentene (30 bar H<sub>2</sub>, 40–60 °C, 45 min), whereas nearly no isomerization to internal alkenes was observed. Upon longer reaction times (4 h), the hydrogenation of internal alkynes to (*Z*)-alkenes proved feasible, however, a hydrogenation of the newly generated alkenes to alkanes was observed at even longer reaction times.

In 2016, Tokmic and Fout reported an *E*-selective semi-hydrogenation of internal alkynes using an NHC-cobalt pre-catalyst, which is converted into the active dihydrogen species *in situ*, and H<sub>2</sub>.<sup>[62]</sup> The origin of the selectivity was explained by the dual role of the catalyst for initial *Z*-selective hydrogenation (Scheme 19, left) as well as subsequent isomerization to the (*E*)-isomer (Scheme 19, right). The semi-hydrogenation has been tested for various substrates, for which generally high *E/Z*-ratios were achieved under mild conditions (1–5 mol% [Co], 4 bar H<sub>2</sub>, 30 °C, 17 h) in moderate to excellent yields (59–96%, Scheme 20).

Similarly, Fu et al.<sup>[63]</sup> used a PNP-pincer cobalt complex for a selective transfer semi-hydrogenation using ammonia borane. With a variation of the PNP-pincer ligand, both a *Z*- and an *E*-

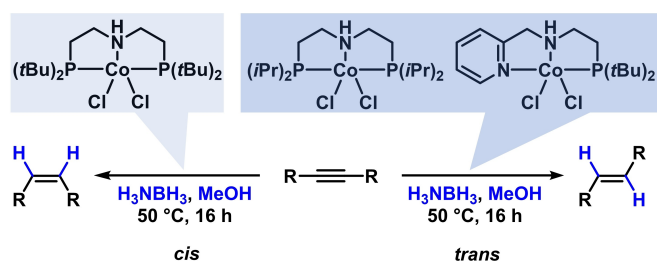


**Scheme 19.** Proposed reaction mechanism for the cobalt-catalyzed *E*-selective semi-hydrogenation, supported by (PHIP)-NMR spectroscopy.<sup>[62]</sup> Left: *Z*-selective semi-hydrogenation; right: *Z*-to-*E*-isomerization of alkenes.



**Scheme 20.** Substrate scope for the cobalt-catalyzed *E*-selective semi-hydrogenation by Tokmic and Fout.<sup>[62]</sup> Isolated yields and *E/Z* ratios are given below each substrate.

selective hydrogenation were possible (Scheme 21). In the initial mechanistic proposal, steric effects due to a difference in bulkiness of the ligands ( $\text{Pr}$  vs.  $\text{tBu}$ ) played an important role. Later detailed mechanistic investigations<sup>[63b]</sup> revealed that the  $\text{tBu}$  ligand could, in fact, promote the isomerization of the (*Z*)-alkene to the (*E*)-alkene as well. However, the isomerization



**Scheme 21.** PNP-pincer cobalt complexes as catalyst precursors for the selective *E*- or *Z*-selective semi-hydrogenation of alkynes.<sup>[63a]</sup>

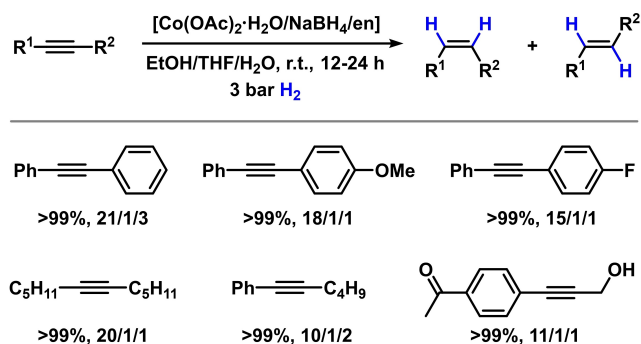
process is hindered due to catalyst deactivation after ligand dissociation of one P-ligand arm.

A 2019 report from Gramigna and co-workers documented that a bimetallic Zr–Co complex is active in the semi-hydrogenation of alkynes.<sup>[64]</sup> Diphenylacetylene was converted primarily to stilbene after 30 h at 23 °C and 1 bar  $\text{H}_2$ , using 10 mol% of the Zr/Co-complex (85 % conversion, 93/7 alkene/alkane, 79/21 *Z/E*). The reaction time could be decreased at elevated temperature, which in turn led to a near complete loss of *Z*-selectivity (60 °C: 3 h, 57/43; 75 °C: 1 h, 51/49). Remarkably, a mechanism for the direct formation of the (*E*)-alkene based on the bimetallic complex was proposed instead of a hydrogenation-isomerization pathway.

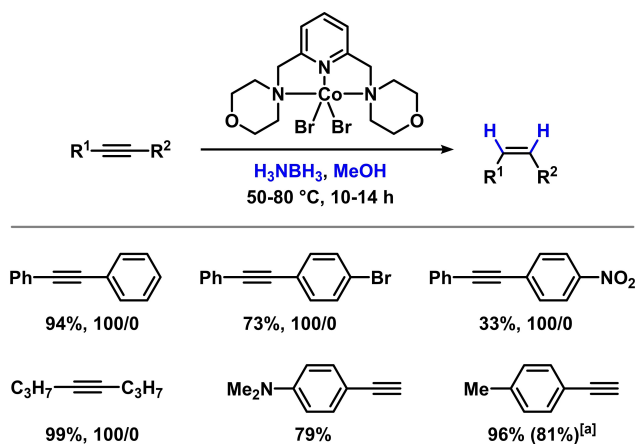
A user-friendly protocol for a *Z*-selective semi-hydrogenation has been developed by Chen et al., using a mixture of cobalt(II) acetate tetrahydrate, sodium borohydride and ethylenediamine in an ethanol/THF/water mixture.<sup>[65]</sup> In the absence of ethylenediamine, full hydrogenation to the alkane was observed. An extensive scope of functionalized substrates was tested with virtually full conversion and high *Z/E* ratios (Scheme 22). This method is especially attractive for practical use, as no prior ligand or complex syntheses is required, paired with mild reaction conditions. Unfortunately, no further mechanistic studies have been carried out.

A phosphine-free NNN-pincer ligand was employed for *Z*-selective transfer semi-hydrogenation of alkynes by Landge and co-workers, using ammonia borane in methanol as the hydrogen source (Scheme 23).<sup>[66]</sup> In the presence of the cobalt complex, ammonia borane is converted into  $\text{B}(\text{OMe})_3$ , releasing hydrogen, which is subsequently incorporated into the alkyne. The solvent methanol was revealed to exhibit a mediating effect on the protonation step, due to monodeuterium incorporation into the alkyne upon usage of  $\text{CD}_3\text{OD}$ . Numerous internal alkynes were selectively converted to the corresponding (*Z*)-alkenes, while practically no formation of (*E*)-alkenes or alkanes was observed in most cases. Moreover, terminal alkynes were successfully converted to terminal alkenes, which could then be further hydrogenated to the alkane upon increasing the reaction temperature and addition of additional ammonia-borane and catalyst.

In a 2016 report by the RajanBabu group, a Co(II) complex bearing a tridentate 2,6-bis(arylimino)pyridine ligand was

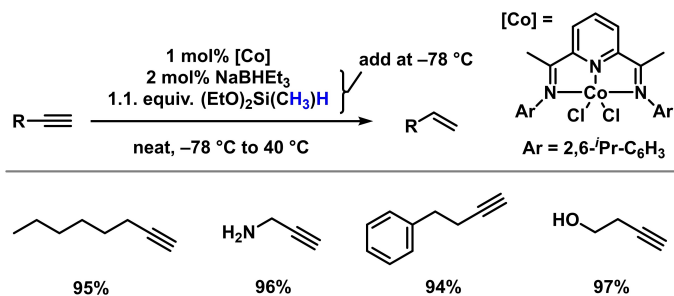


**Scheme 22.** Substrate scope for a semi-hydrogenation protocol based on cobalt catalysis.<sup>[65]</sup> Conversions and *Z/E*/alkane ratios given below substrates.



**Scheme 23.** An NNN-pincer cobalt complex for the semi-hydrogenation of alkynes.<sup>[66]</sup> Isolated yields and *Z/E* ratios given below each substrate. [a] Yield of alkanes after addition of 4 mol% [Co] and additional ammonia-borane at elevated temperature and longer reaction time.

employed in the reduction of terminal alkynes and alkenes using (EtO)<sub>2</sub>Si(Me)H as hydrogen source and a catalytic amount of NaBHET<sub>3</sub> (Scheme 24).<sup>[67]</sup> While primarily developed for the reduction of alkenes to alkanes, the reduction of alkynes can be controlled toward selective alkene formation by the silane stoichiometry. The catalytically active Co species is presumably generated by addition of NaNHET<sub>3</sub> at -78 °C, the silane is then introduced and the mixture is gradually warmed. Mechanistic investigations strongly suggested that both H atoms originate from the silane, as the use of deuterated solvents or the presence of D<sub>2</sub>O did not effect deuterium incorporation. Additionally, the product yields roughly corresponded to the equivalents of silane when sub-stoichiometric amounts were used. The authors proposed initial formation of a hydridocobalt(I) species by NaBHET<sub>3</sub>, followed by the insertion of the alkyne into Co-H. Reaction with the silane affords the alkene and a Co-Si species, which regenerates the Co(II) hydride and forms polymeric siloxanes. Only four terminal aliphatic alkynes were reported; functional groups such as bromides, alcohols, amines, carbonyls and epoxides were tolerated under the conditions; yields were consistently excellent (generally > 90%).

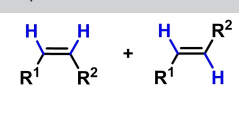
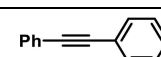
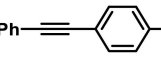
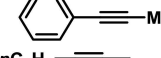
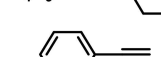
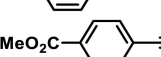
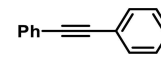
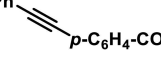
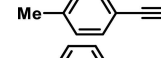
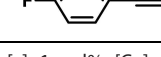
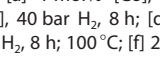


**Scheme 24.** Cobalt-catalyzed reduction of terminal alkynes by RajanBabu and coworkers.<sup>[67]</sup>

In 2017, a heterogeneous cobalt catalyst capable of a *Z*-selective semi-hydrogenation of both internal and terminal alkynes using hydrogen gas was developed by Chen et al.<sup>[68]</sup> The cobalt catalyst was prepared via pyrolysis of a Co(OAc)<sub>2</sub>/phenanthroline mixture in the presence of SiO<sub>2</sub> as solid support. The thus synthesized cobalt nanoparticles were encapsulated in an N-doped graphene layer and were used to hydrogenate various different internal alkynes (Table 3, top). A similar report from the same year also utilized N-graphitic modified (NGR) cobalt nanoparticles.<sup>[69]</sup> In this process, ammonia borane was used as the hydrogen source, allowing for milder reaction conditions and thus a minimization of potential isomerization reactions occurring at elevated temperatures. Again, internal and terminal alkynes were selectively converted. Additionally, it was demonstrated that the heterogeneous Co catalyst could be reused after filtration without loss of activity or selectivity for up to nine cycles (Table 3, bottom).

In 2019, a cobalt-catalyzed transfer semi-hydrogenation using water as the hydrogen source was reported by Li et al.<sup>[70]</sup> The combination of cobalt(II) iodide with 3 equiv. Zn metal in the presence of 10 equiv. H<sub>2</sub>O in methanol led to the formation of predominantly (*Z*)-alkenes at 60 °C in generally high yields and selectivities. A noteworthy modification of this system included the use of the ligand dppe (1,2-bis(diphenylphosphino)ethane) and the change of the solvent

**Table 3.** Heterogeneous N-graphitic cobalt catalysts for the hydrogenation of internal and terminal alkynes. Entries 1–6,<sup>[68]</sup> entries 7–10.<sup>[69]</sup>

$R^1 \equiv R^2 \xrightarrow[\text{[H]-source conditions}]{\text{[Co]}}$ 				
<b>A:</b> 1–4 mol% Co/phen@SiO <sub>2</sub> , MeCN, 120 °C, H <sub>2</sub> <b>B:</b> 4 mol% Co@NGR, MeOH, 80 °C, 1.2 equiv. H <sub>3</sub> NBH <sub>3</sub>				
Entry	Alkyne	Cond.	Alkene [%]	<i>Z/E</i>
1 <sup>[a]</sup>		A	98 (96) <sup>[b]</sup>	9/1 (9/1) <sup>[b]</sup>
2 <sup>[c]</sup>		A	95	6/1
3 <sup>[a]</sup>		A	99	1.5/1
4 <sup>[d]</sup>		A	63	mostly <i>Z</i> + isomers
5 <sup>[a]</sup>		A	73	4% alkane
6 <sup>[e]</sup>		A	66	13% alkane
7 <sup>[f]</sup>		B	93	100/0
8 <sup>[f]</sup>		B	90	100/0
9 <sup>[g]</sup>		B	99	-
10 <sup>[g]</sup>		B	99	-

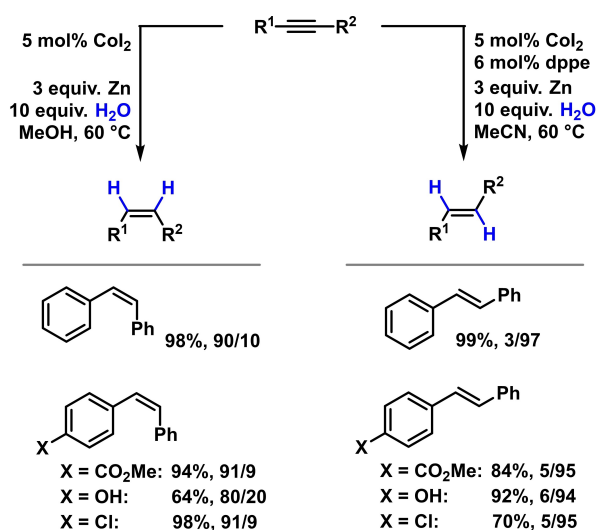
Conditions: [a] 1 mol% [Co], 30 bar H<sub>2</sub>, 15 h; [b] after three runs; [c] 3 mol% [Co], 40 bar H<sub>2</sub>, 8 h; [d] 4 mol% [Co], 40 bar H<sub>2</sub>, 10 h; [e] 1 mol% [Co], 30 bar H<sub>2</sub>, 8 h; 100 °C; [f] 24 h; [g] 18 h.

from methanol to acetonitrile. Using these modifications, the diastereoselectivity switched from (*Z*)- to (*E*)-alkenes (Scheme 25). Mechanistic proposals for both systems feature an initial reduction of the Co(II) center (in Co<sub>2</sub>) to a Co(I) species by Zn, to which the alkyne can subsequently coordinate in preparation for the hydrogenation step. The *E*-selectivity was hypothesized to result from steric hindrance of the ligand and from direct isomerization during the hydrogenation step. No isomerization was observed from free (*Z*)-alkenes to (*E*)-alkenes in control experiments.

Bimetallic nanoparticles featuring cobalt and aluminium have been reported to fully hydrogenate terminal alkynes by Schmolke et al.<sup>[71]</sup> However, in the presence of coordinating groups *para* to the alkynyl substituent, semi-hydrogenated products are obtained, likewise when the reaction time is shortened. One internal alkyne has been hydrogenated under the same reaction conditions, leading to the (*Z*)-alkene as the major product.

A recent study by the group of Petit<sup>[72]</sup> used the commercial Co(I) precursor [CoCl(PPh<sub>3</sub>)<sub>3</sub>] to generate cobalt nanoparticles via disproportionation in THF. Rapid agglomeration and subsequent deactivation of the catalyst was inhibited by the addition of fatty alcohols. The nanoparticles were probed for the semi-hydrogenation of internal alkynes, leading to mainly (*Z*)-alkenes. Alkynes featuring coordinating groups such as alcohols instead delivered mainly the (*E*)-alkenes and considerably higher amounts of fully hydrogenated alkanes. The coordinating groups allow for strong binding to the Co-NP surface, resulting in a longer contact time with the catalytically active site and thus in the full hydrogenation of the (*Z*)-alkenes to alkanes, while the (*E*)-alkenes were mostly preserved. A reduction of H<sub>2</sub> pressure evaded the formation of alkanes and retained the *Z*-selectivity, albeit with lower overall conversion.

An innovative visible-light-driven transfer semi-hydrogenation was reported in 2020 by Tian and co-workers.<sup>[73]</sup> The



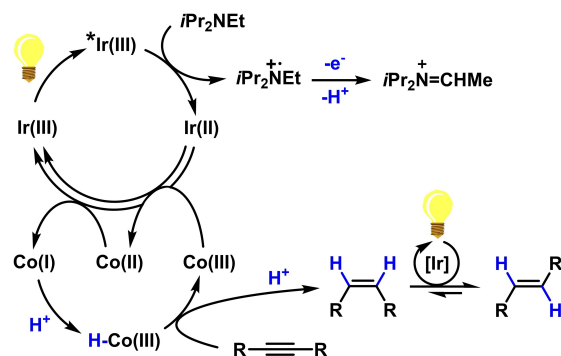
**Scheme 25.** Transfer semi-hydrogenation of internal alkynes to (*Z*)-alkenes (left) and (*E*)-alkenes (right). <sup>1</sup>H-NMR yields vs. 1,3-benzodioxole and *Z/E* ratios are given.<sup>[70]</sup>

photo-catalytic system revolves around an Ir(III) photocatalyst, which can oxidize the formal hydride source diisopropylethylamine upon photoexcitation to generate an Ir(II) species and an iminium ion after formal elimination of a hydrogen radical. The Co(II) from the cobalt source is subsequently reduced by Ir(II), closing the photocatalytic cycle and leading to Co(I). Protonation results in a Co(III) hydride, which can *Z*-selectively hydro-metallate the alkyne; protodemetalation and two-fold reduction of the Co(III) species in two separate photocatalytic cycles re-forms the Co(I) species while the (*Z*)-alkene is isomerized to the (*E*)-alkene under photocatalytic conditions (Scheme 26). Cobalt(II) bromide paired with tri-*n*-butylphosphine was used as the cobalt source, while acetic acid was employed as the proton source. After 14 h at room temperature, several terminal and internal alkynes were converted to the alkene products in high yields. However, due to the photocatalytic *E/Z*-isomerization being an equilibrium reaction, the *Z/E*-ratios obtained by this method were low (approx. 70/30 in most cases).

A potential industrial/technical application for the semi-hydrogenation of propyne to propene has been achieved with N-doped carbon nanotubes on Ti<sub>3</sub>C<sub>2</sub> sheets, embedded with cobalt nanoparticles.<sup>[74]</sup> Propyne could selectively be hydrogenated to propene with a selectivity of ~96% while achieving practically full conversion.

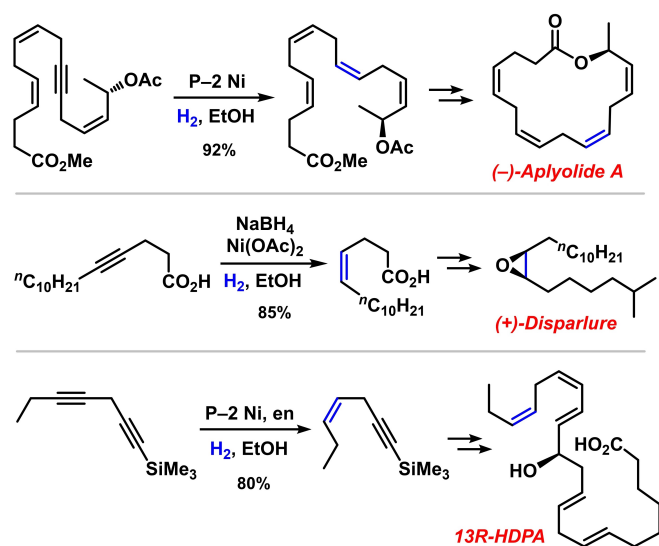
## 9. Nickel<sup>[11,27,75,76]</sup>

The earliest report for a *Z*-selective semi-hydrogenation using nickel was the usage of “P-2 Nickel” by Herbert Brown in 1963,<sup>[77]</sup> only 11 years after Lindlar’s original publication.<sup>[7b]</sup> A colloidal black catalyst was obtained after reduction of Ni(OAc)<sub>2</sub> with sodium borohydride in ethanol. Addition of ethylenediamine improved the selectivity of the reaction. A handful of alkynes were hydrogenated with near-exclusive formation of the (*Z*)-alkenes in high yields under mild conditions (1 bar H<sub>2</sub>, room temperature). The “P-2 Ni” method of (semi-)hydrogenation is relatively well-established and has found widespread applications in synthetic chemistry. These include, among others, the total synthesis of the macrolide aplyolide A,<sup>[78]</sup> the gypsy moth pheromone disparlure,<sup>[79]</sup> the hydroxylated

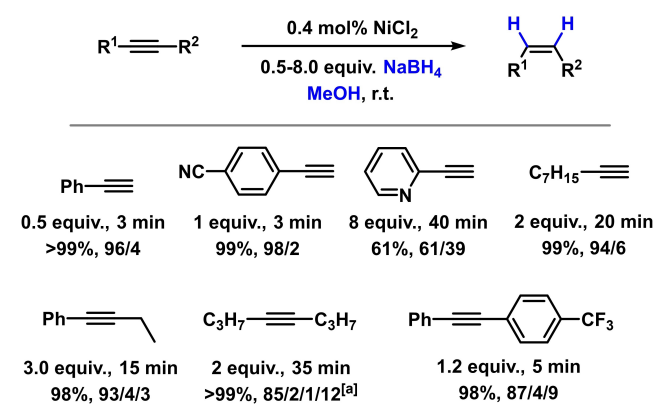


**Scheme 26.** The hypothesized catalytic cycles involved in the photochemical transfer semi-hydrogenation of alkynes.<sup>[72]</sup>

polyunsaturated carboxylic acid 13R-HDPA as a biochemical precursor to resolvins<sup>[80]</sup> as well as several other examples (Scheme 27).<sup>[81]</sup> The P-2 nickel protocol is undoubtedly popular in complex molecule synthesis, not least because of its long history, operational simplicity and high accessibility due to the cheap, commercially available reagents being employed. This method generally delivers exceptional *Z*-selectivities in lightly functionalized molecules, however the yields and functional group tolerance are mediocre. This necessitates careful planning of the synthetic route to include the corresponding step as early as possible. For instance, whereas alcohols, esters, acetals, benzylic ethers, and carboxylic acids are tolerated, aryl halides undergo facile hydrodehalogenation.<sup>[81d]</sup> Occasionally, mixtures of unreacted starting material, (*Z*)-alkene and alkane are observed after consumption of 1 equiv. H<sub>2</sub>.<sup>[81j]</sup> In other cases, the chemoselectivity might be higher, as shown impressively by the semi-hydrogenation of hepta-1,4-diyne-1-yl-trimethylsilane



**Scheme 27.** Application of P-2 Ni in the total syntheses of (-)-aplyolide A,<sup>[78]</sup> (+)-disparlure<sup>[79]</sup> and 13R-HDPA ((R)-13-hydroxy-7Z,10Z,13R,14E,16Z,19Z-decosapentaenoic acid).<sup>[80]</sup> en = ethylene-1,2-diamine.



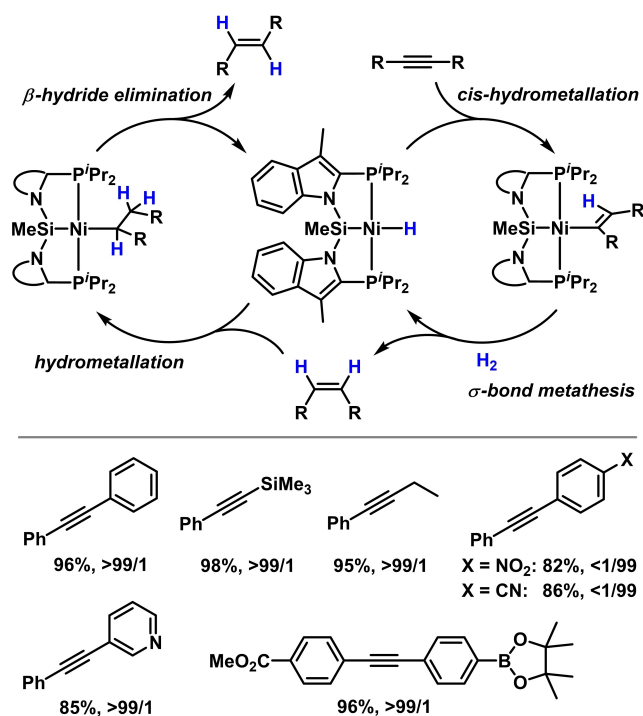
**Scheme 28.** A simple nickel-catalyzed transfer semi-hydrogenation protocol for terminal and internal alkynes.<sup>[82]</sup> Conversions and product selectivities (*Z*/*E*/alkane) are given below each substrate. [a] 12% 4-octanol formed.

as an intermediate step in the synthesis of 13R-HDPA (Scheme 27, bottom).<sup>[80]</sup> The catalyst is able to discriminate between the alkyl- and the trimethylsilyl-substituted alkyne to selectively reduce the alkyl-substituted triple bond.

A similar transfer hydrogenation system was reported in 2017 by Wen and co-workers.<sup>[82]</sup> In this user-friendly protocol, the authors reduced NiCl<sub>2</sub> in methanol using NaBH<sub>4</sub> to form nickel nanoparticles, which were characterized via TEM (average particle diameter: 6.2 ± 0.3 nm). The hydrogen atoms incorporated into the alkyne during the hydrogenation step originate from both the reductant NaBH<sub>4</sub> (as hydride) as well as methanol (as proton), which was proven by deuteration experiments. Low amounts of nickel (0.4 mol%) and 0.5–8.0 equiv. of NaBH<sub>4</sub> were sufficient for a quantitative conversion to the (*Z*)-alkenes within minutes at room temperature (Scheme 28).

Very recently, Hale and co-workers reported a diastereoselective semi-hydrogenation using molecular hydrogen at ambient pressure and a nickel complex featuring a PSiP pincer ligand.<sup>[83]</sup> In most cases, (*E*)-alkenes were obtained from the respective alkynes. For alkynes bearing electron-deficient aryl substituents, the selectivity switched towards the (*Z*)-isomer (Scheme 29). The authors propose a (*Z*)-selective semi-hydrogenation cycle in combination with a separate *E/Z* isomerization cycle via a hydrometallation/ $\beta$ -hydride elimination pathway.

The application of nickel nanoparticles as hydrogenation “catalysts” without hydrogen gas was previously shown by Alonso et al.<sup>[84]</sup> The Ni-nanoparticles were prepared via reduction of NiCl<sub>2</sub> with 4 equiv. lithium in the presence of a catalytic amount of 4,4'-di-*tert*-butylbiphenyl as electron carrier in THF.



**Scheme 29.** Stereoselective Ni-catalyzed semi-hydrogenation of internal alkynes with H<sub>2</sub>.<sup>[83]</sup> Conditions: 1–2.5 mol% [Ni], 1 bar H<sub>2</sub>, benzene-d<sub>6</sub> (0.1 M), r.t., 4 h. <sup>1</sup>H-NMR yields and *E/Z* ratios are given below each substrate.

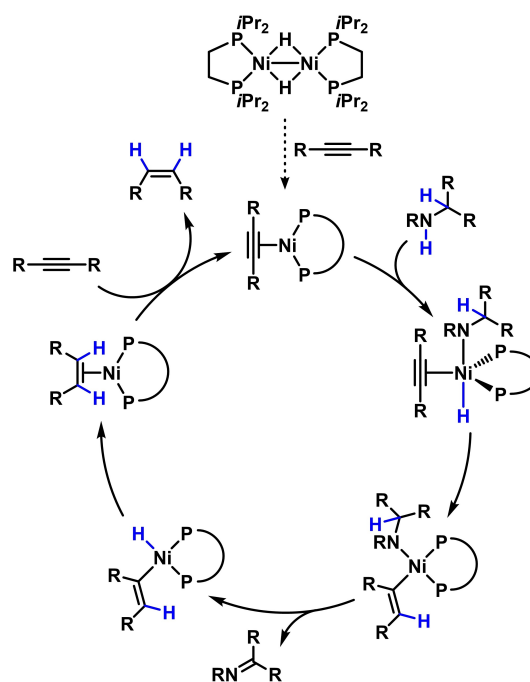
Two equivalents of ethanol or isopropanol were added as the hydrogen source for the semi-hydrogenation step. This method requires the use of stoichiometric or superstoichiometric amounts of Ni and Li, which poses a major drawback.

Additional nickel-catalyzed transfer semi-hydrogenation systems have been reported that utilize silane/water or methanol,<sup>[85]</sup> amines,<sup>[86]</sup> phosphinic acid,<sup>[87]</sup> or zinc/formic acid<sup>[88]</sup> as hydrogen sources.  $[\text{Ni}(\eta^2\text{-C,C-alkyne})(\text{dippe})]$  complexes have been employed by Barrios-Francisco and García for the semi-hydrogenation of internal alkynes in 2009.<sup>[85]</sup> The complexes were formed using the dimeric  $[\text{NiH}(\text{dippe})]_2$  as precursor. Reduction of the alkyne in a stoichiometric nickel-mediated reaction yielded the (*Z*)-alkene in the presence of water and the (*E*)-alkene in the presence of methanol as hydrogen sources. The phosphine ligand is oxidized irreversibly during the course of this reaction, thus preventing a catalytic application. This drawback could be circumvented with the addition of triethylsilane as an oxygen scavenger and hydrogen source. No silane was required when methanol was used as the hydrogen source due to the potential oxidation of methanol to formaldehyde. High reaction temperatures (180 °C) and long reaction times (48 h) were required for the reductions (shorter reaction times were possible for the reactions with methanol). Only limited mechanistic details were provided, particularly the origin of the *E*- or *Z*-selectivity with different hydrogen sources remained unclear.

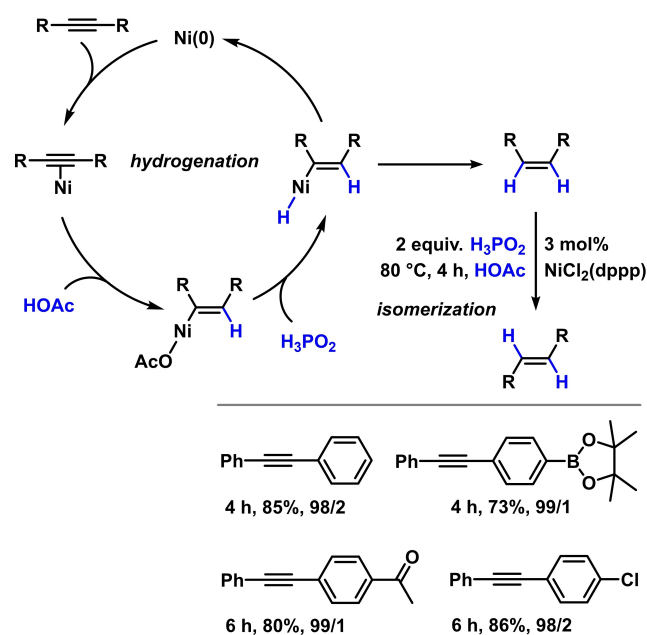
The same group later reported a similar system based on the  $[\text{NiH}(\text{dippe})]_2$  complex using amines as the hydrogen source.<sup>[86]</sup> High temperatures (180 °C) and long reaction times (72 h) were necessary for the desired outcome of the reaction; the nature of the solvent (coordinating or non-coordinating) as well as the amine also played a crucial role in the conversion and selectivity. The (*E*)-alkene was the main product in most cases. An initial formation of the (*Z*)-alkene and subsequent isomerization under the reaction conditions was proposed as the main pathway (Scheme 30).

In 2014, Chen et al. reported the use of phosphinic acid as the hydrogen source, paired with  $[\text{NiCl}_2(\text{dppp})]$  (dppp = 1,3-bis-(diphenylphosphine)propane) in acetic acid for an (*E*)-selective semi-hydrogenation of internal alkynes.<sup>[87]</sup> It was hypothesized that Ni(0) is operating as the catalytically active species (Scheme 31, top). After initial formation of the (*Z*)-alkene in the transfer hydrogenation step, the alkene undergoes a subsequent isomerization to its (*E*)-alkene, as demonstrated with isomerization experiments (Scheme 31, middle). Near-exclusive formation of the (*E*)-alkenes was observed for most substrates in high yields after 4–48 h of reaction time (Scheme 31, bottom).

A transfer hydrogenation protocol that enables access to both the (*E*)- and (*Z*)-isomer by variation of the nickel catalyst has been developed by Richmond and Moran in 2015.<sup>[88]</sup> Zinc in combination with formic acid was employed as the hydrogen source, hydrogenating internal alkynes at 120 °C in dioxane. To achieve a *Z*-selective semi-hydrogenation,  $\text{NiBr}_2$  was used as the precursor, whereas  $[\text{NiCl}_2(\text{dme})]$  (dme = 1,2-dimethoxyethane) combined with triphos (bis(diphenylphosphinoethyl)phenylphosphine) gave predominantly (*E*)-alkenes (Scheme 32). These

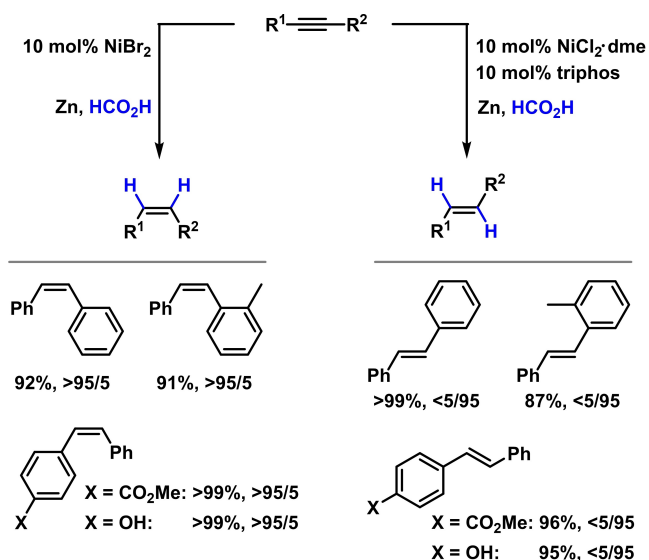


**Scheme 30.** Proposed mechanism for the initial formation of the (*Z*)-alkene with a  $[\text{NiH}(\text{dippe})]_2$  pre-catalyst. The  $[\text{Ni}(\text{dippe})(\eta^2\text{-DPA})]$  (DPA = diphenylacetylene) was isolated and characterized by X-ray crystallography.<sup>[86]</sup>

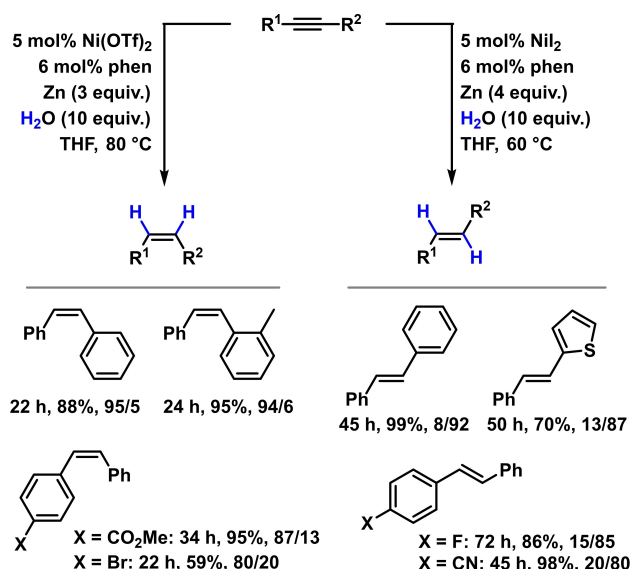


**Scheme 31.** An *E*-selective nickel-catalyzed transfer semi-hydrogenation of internal alkynes using phosphinic acid as the hydrogen source.<sup>[87]</sup> Reaction times, isolated yields and *E/Z* ratios are given below each substrate.

starkly different reaction outcomes are rationalized by an inherently *Z*-selective semi-hydrogenation by means of either nickel catalyst, whereas the presence of triphos enables an additional *Z*-to-*E*-isomerization cycle. Mechanistic insight was gained by isomerization experiments: (*Z*)-Stilbene underwent



**Scheme 32.** A nickel-catalyzed transfer semi-hydrogenation yielding (*Z*)- or (*E*)-alkenes.<sup>[88]</sup> Reaction conditions: 5 equiv. Zn, 5 equiv. HCO<sub>2</sub>H, dioxane, 120 °C, 16 h. Isolated yields and *Z/E* ratios are given below each substrate.



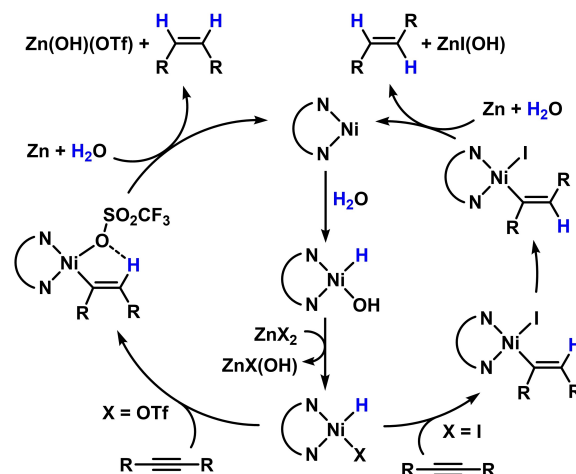
**Scheme 33.** Scope of the nickel-catalyzed semi-hydrogenation reported by Li and co-workers in 2021, affording (*Z*)- or (*E*)-alkenes.<sup>[89]</sup> Reaction times, <sup>1</sup>H-NMR yields vs. 1,3-benzodioxole and *Z/E* ratios are given below each substrate.

complete isomerization to (*E*)-stilbene in the presence of [NiCl<sub>2</sub>(dme)] and triphos within 1 h at 120 °C, while no isomerization was observed when only NiBr<sub>2</sub> was present.

A similar reaction featuring excess zinc in H<sub>2</sub>O as the hydrogen source was reported six years later by Li et al.<sup>[89]</sup> In the presence of 1,10-phenanthroline and 5 mol% Ni(OTf)<sub>2</sub>, aryl- or alkyl-substituted alkynes were converted to primarily (*Z*)-alkenes after 22–36 h at 80 °C in THF. The use of NiI<sub>2</sub> instead altered the selectivity towards (*E*)-alkenes at slightly lower temperatures and longer reaction times (60 °C, 40–72 h, Scheme 33). As (*Z*)-stilbene was not isomerized to (*E*)-stilbene under the latter conditions, the authors ruled out a stepwise hydrogenation-isomerization mechanism and hypothesized that the intermediate vinyl-Ni complex, obtained after *cis*-selective hydrometallation of the alkyne, undergoes direct isomerization without formation of intermediate (*Z*)-alkene. This isomerization is hypothesized to be hindered in the presence of coordinating triflate due to the formation of intramolecular hydrogen bonds (Scheme 34).

An alternative example for a nickel-catalyzed system with switchable selectivity was reported in 2019 by Murugesan and co-workers.<sup>[90]</sup> Nickel(II) nitrate hexahydrate was used as nickel source; exclusive use of this salt in acetonitrile at 30 bar H<sub>2</sub> and 120 °C gave a heterogeneous catalyst for *Z*-selective semi-hydrogenation of internal and terminal alkynes (selectivities up to 99/1), a small amount of alkanes being observed for the latter. In the presence of multidentate ligands such as triphos, mostly (*E*)-alkenes were observed. A homogeneous nickel catalyst was hypothesized in this case, as the ligand is able to stabilize the intermediate nickel hydride species. A hydrogenation-isomerization mechanism was suggested (Scheme 35).

A further improvement in the field of *E*-selective semi-hydrogenation was contributed by Thiel et al.,<sup>[91]</sup> where NiI<sub>2</sub> or Ni(OTf)<sub>2</sub> in combination with dppf (1,1'-bis(diphenylphosphino)-



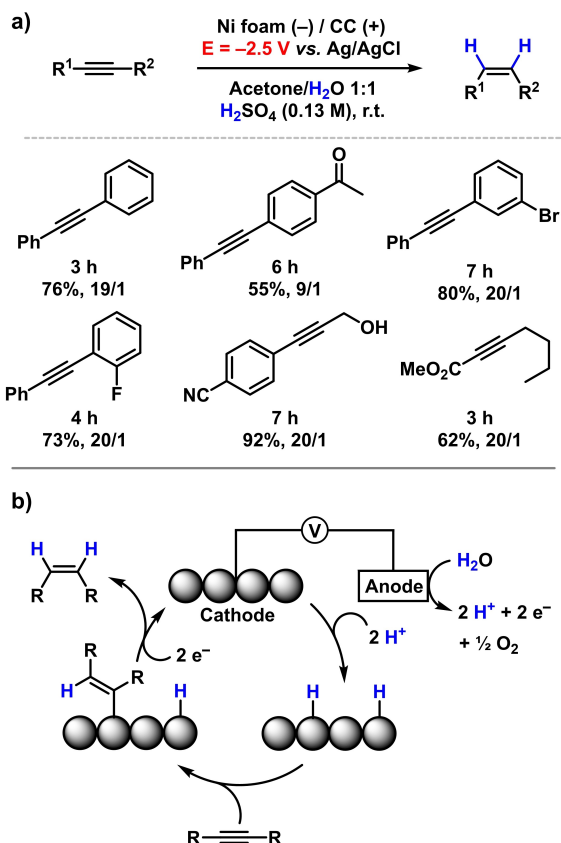
**Scheme 34.** Proposed divergent mechanisms of the semi-hydrogenation shown in Scheme 30 above depending on the anion.<sup>[89]</sup>

ferrocene) as ligand offered a generally applicable catalytic protocol for the synthesis of (*E*)-alkenes. Under similar conditions to the triphos-system (30 bar H<sub>2</sub>, 100 °C, dioxane, 16 h),<sup>[90]</sup> a multitude of alkynes were selectively hydrogenated, most remarkably including alkyl-substituted alkynes, which have not been previously successfully hydrogenated. A similar hydrogenation-isomerization mechanism is postulated.

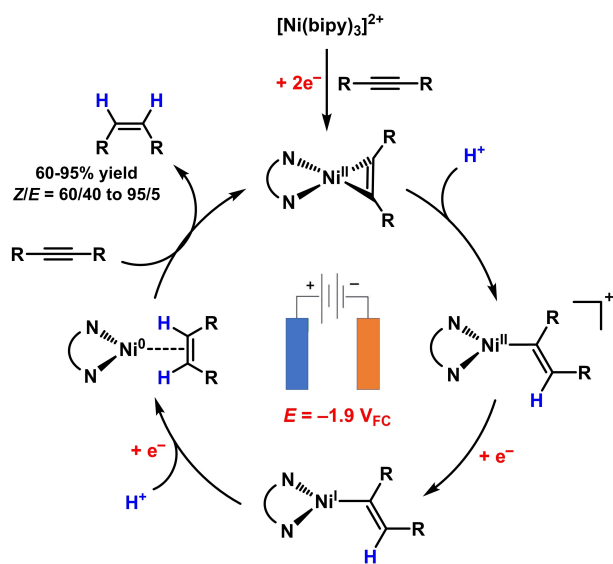
Akin to the iron-nanoparticle-catalyzed semi-hydrogenation in ionic liquids (see chapter 7),<sup>[50]</sup> a very related system containing nickel nanoparticles was later reported by Konnerth and Precht.<sup>[92]</sup> The nickel nanoparticles were directly prepared via thermal decomposition of [Ni(cod)<sub>2</sub>] (cod = 1,5-cyclooctadiene) in the nitrile-containing ionic liquid. Compared to the







**Scheme 37.** a) Substrate scope of the electrochemical Z-selective semi-hydrogenation of internal alkynes using a Ni foam cathode.<sup>[95]</sup> CC = carbon cloth. Reaction times, <sup>1</sup>H-NMR yields vs. 2,3,5,6-tetrachloronitrobenzene and Z/E ratios are given below each substrate. b) Proposed mechanism for the electrochemical Z-selective semi-hydrogenation of internal alkynes using a Ni foam cathode.<sup>[95]</sup>



**Scheme 38.** Electrochemical nickel-catalyzed semi-hydrogenation of alkynes by sequential protonation-reduction events.<sup>[96]</sup>

The local electrostatic fields within the zeolite structure in combination with the nickel were hypothesized to induce heterolytic dihydrogen cleavage.

The pyrolysis of  $\text{Ni}(\text{OAc})_2 \cdot 4 \text{H}_2\text{O}$  in the presence of melamine yielded  $\text{Ni}_3\text{N}$  nanorods on an N-doped carbon solid support, as was reported by Shi and co-workers in 2020.<sup>[98]</sup> Terminal and internal alkynes were successfully semi-hydrogenated in a Z-selective fashion (Table 4). Sensitive functional groups such as carbonyls, esters or alcohols were well tolerated under the reaction conditions. As a downside, rather high catalyst loadings (7.8 mol%) and elevated  $\text{H}_2$  pressures (20 bar) were required.

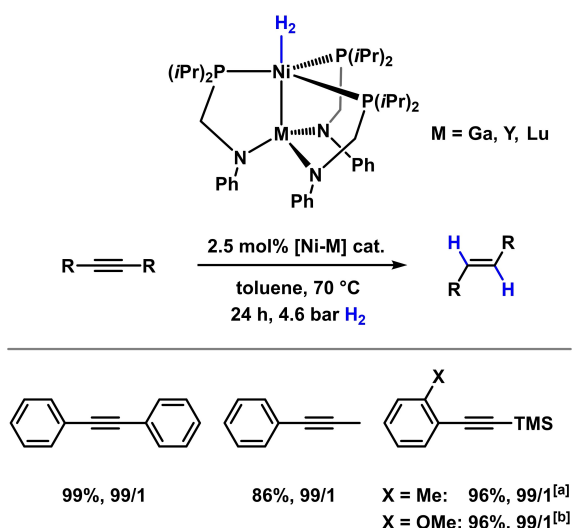
In 2020, nickel-containing bimetallic heterogeneous catalysts were reported to be effective for semi-hydrogenation of alkynes.<sup>[99,100]</sup> Ramirez and Lu utilized nickel combined with rare earth metals (Ga, La, Y, Lu) for E-selective hydrogenation.<sup>[96]</sup> Comparatively mild reaction conditions were possible (Scheme 39). Only a limited substrate scope with few functional groups was reported, however, a detailed kinetic and mechanistic investigation was presented by the authors (Scheme 40). Depending on the metal the nickel is combined with (electronic and steric effects, Lewis acidity), different reaction pathways have been identified. The rare earth metal functions as a promoter that alternates electronic characteristics of the nickel center and thus influences the substrate binding properties of the catalyst while additionally providing a free coordination site for the phosphine ligand. The latter is a crucial feature, as the nickel center requires a free coordination site in order to coordinate the alkyne, which is enabled by the transfer of a phosphine ligand from the Ni to the rare earth metal.

The second example of a bimetallic nickel catalyst includes polyvinylpyrrolidone-stabilized nickel-iron nanoparticles that were prepared by reduction of  $\text{NiCl}_2 \cdot 6 \text{H}_2\text{O}$  and  $\text{FeSO}_4 \cdot 7 \text{H}_2\text{O}$  in aqueous solution using  $\text{NaBH}_4$ .<sup>[100]</sup> Different Ni-to-Fe ratios have been prepared and investigated: While the pure iron catalyst

**Table 4.** Solid-supported  $\text{Ni}_3\text{N}$  nanorods as catalyst for the Z-selective semi-hydrogenation of terminal and internal alkynes.<sup>[98]</sup>

Entry	Alkyne	Time [h]	Conversion (alkene) [%]	Z/E
1		1	> 98 (87)	-
2		5	99 (98)	98/2
3 <sup>[a]</sup>		15	> 99 (96)	95/5
4		3	> 99 (89)	95/5
5 <sup>[b]</sup>		11	> 99 (99)	> 99/ 1
6	$n\text{C}_3\text{H}_7 \equiv n\text{C}_3\text{H}_7$	2	> 99 (96)	> 99/ 1

Conditions: [a] 120 °C, 30 bar  $\text{H}_2$ ; [b] 120 °C, 40 bar  $\text{H}_2$ .



**Scheme 39.** Ni–M-bimetallic catalysts for *E*-selective semi-hydrogenation of internal alkynes.<sup>[99]</sup> <sup>1</sup>H-NMR yields vs. 1,3,5-trimethoxybenzene and *E/Z* ratios for M = Y are given below each substrate. [a] 60 h; [b] 3.5 mol% catalyst.

was inactive under the aqueous reaction conditions, the pure nickel and the bimetallic Ni<sub>1</sub>Fe<sub>1</sub> and Ni<sub>3</sub>Fe<sub>1</sub> catalysts gave primarily alkanes. With a Fe/Ni ratio of 3:1, the Ni<sub>1</sub>Fe<sub>3</sub> catalyst showed highest semi-hydrogenation activity, which could be further improved towards higher *Z*-selectivities with further optimization and screening of additives. The addition of *n*-butylamine and the iron content in the nanoparticles are essential for regulating the free adsorption sites for alkenes to prevent overreduction and improving the chemoselectivity.

## 10. Copper<sup>[11,27,101–104]</sup>

Interestingly, most examples of powerful copper-catalyzed semi-hydrogenations of alkynes have emerged in the last decade. One of the pioneering reports for a direct semi-hydrogenation using dihydrogen was published by Semba et al. in 2015.<sup>[105]</sup> Simple copper(I) salts, such as CuCl in combination with phosphine ligands (PPh<sub>3</sub>), were used in the presence of alkoxides (LiO<sup>*t*</sup>Bu) and a proton source (<sup>*i*</sup>PrOH). A straightforward mechanism involving a heterolytic cleavage of the hydrogen followed by *cis*-hydrocupration of the alkyne and final protonolysis of the vinyl copper species has been suggested (Scheme 41). Another related method utilized tethered alkoxydycopper(I) complexes formed *in situ* as catalysts for a highly *Z*-selective semi-hydrogenation of internal alkynes without over-reduction.<sup>[106]</sup> NHC ligands bearing an alkoxide group were used as ligands to avoid the use of protic additives and additional alkoxides. An intramolecular heterolytic hydrogen bond cleavage was proposed to occur under the reaction conditions, forming a copper hydride species and a free alcohol group (Scheme 42), analogous to the mechanism depicted in Scheme 41. Further improvements were made with other NHC ligands by the same group. Use of the IPr ligand gave an air-stable NHC-copper(I) hydroxide complex for *Z*-selective semi-

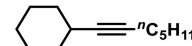
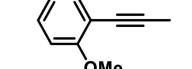
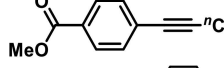
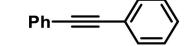
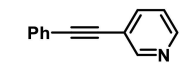
hydrogenation that circumvents the need for preactivation.<sup>[107]</sup> However, elevated hydrogen pressures (up to 100 bar) are necessary (Scheme 43).

An alternative approach was presented in 2016 in a report by Wakamatsu et al.<sup>[108]</sup> The authors employed [Cu(O<sup>*t*</sup>Bu)(SIMes)] as the catalyst for a *Z*-selective semi-hydrogenation, generated *in situ* from [CuCl(SIMes)] and NaO<sup>*t*</sup>Bu in an octane/dioxane mixture (Table 5). This system functioned under atmospheric hydrogen pressure, albeit at elevated temperatures (100 °C). Esters were well tolerated, but no desired product was obtained in the presence of an aromatic bromide or nitrile.

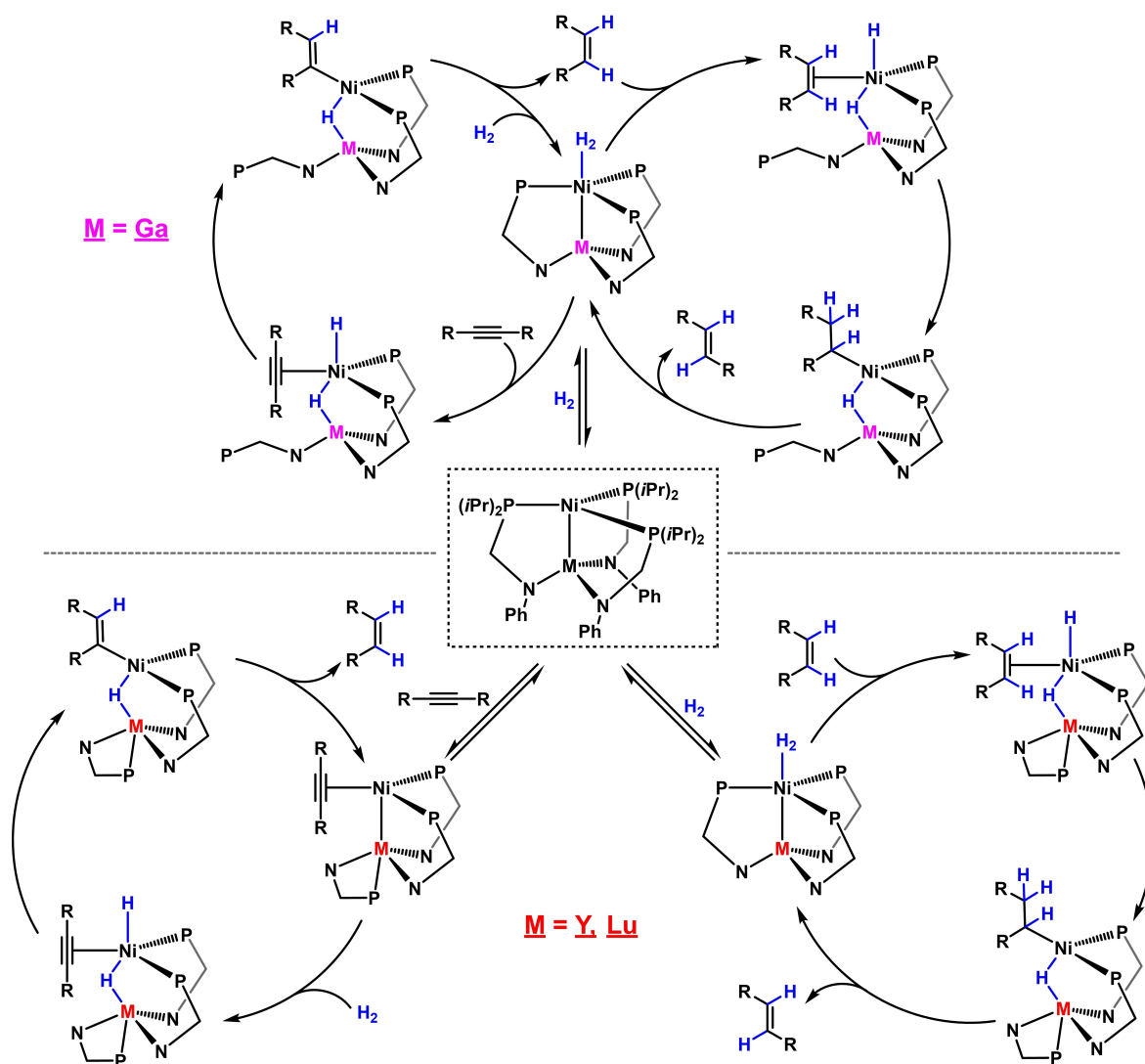
Similar to the bimetallic Fe-catalyst reported by Karunananda and Mankad (see chapter 7), a copper analogue of the same catalyst for the *E*-selective semi-hydrogenation of alkynes was reported.<sup>[56]</sup>

Silica-supported copper nanoparticles were described extensively as heterogeneous catalysts by the Copéret group.<sup>[109]</sup> The immobilized copper nanoparticles were prepared by the treatment of SiO<sub>2</sub> with the mesitylcopper(I) pentamer in toluene and subsequent hydrogenation at 300 °C.<sup>[109a]</sup> The catalyst was assessed for a variety of different alkynes, yielding only low selectivities for some substrates. This drawback was averted by the use of tricyclohexylphosphine (PCy<sub>3</sub>) as the ligand: With this modification, both high yields and *Z*-selectivities were achieved. Detailed mechanistic experiments were reported in order to evaluate the influence of the ligand.<sup>[109b,c]</sup> Parahydrogen-induced polarization experiments (PHIP)<sup>[109b]</sup> showed the feasibility of pairwise hydrogen addition on the surface with a significant influence of the PCy<sub>3</sub> ligand (0.2–0.6% pairwise hydrogen addition to 1-butyne without PCy<sub>3</sub> and ≥2.7% with PCy<sub>3</sub>). This result and the increased selectivity in the presence of the ligand were explained by a selective binding of the phosphine ligand

**Table 5.** [Cu(O<sup>*t*</sup>Bu)(SIMes)]-catalyzed *Z*-selective semi-hydrogenation of internal alkynes.<sup>[108]</sup>

Entry	Alkyne	Alkene [%] <sup>[a]</sup>	<i>Z/E</i>
1		68	> 99/1
2		60	97/3
3 <sup>[b]</sup>		66	93/7
4		80	92/8
5		88	90/10

[a] Isolated yields; [b] CuCl used instead of [CuCl(SIMes)].

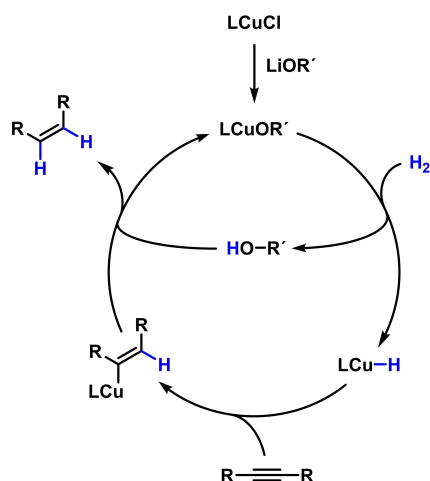


**Scheme 40.** Mechanistic proposals for *E*-selective semi-hydrogenation of alkynes with bimetallic nickel-M catalysts (M = Ga, Y, Lu): Hydrogenation (left) and *E*/*Z*-isomerization (right).<sup>[99]</sup> Ph, iPr groups on N and P atoms are omitted for clarity. Top: Ni–Ga catalyst; H<sub>2</sub> coordinates to Ni, followed by alkyne coordination; phosphine ligand then dissociates. Bottom: Ni–M catalysts (M = Y, Lu); alkyne is coordinated first, followed by oxidative addition of H<sub>2</sub> and phosphine coordination to M.

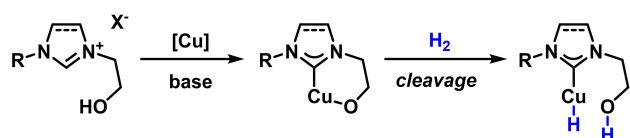
to catalytically active, but more unselective sites. The coordination of PCy<sub>3</sub> on the surface also impedes the migration and scrambling of coordinated hydrogen. With further adsorption and kinetic experiments,<sup>[109c]</sup> it was shown that both alkynes and phosphine ligands, possess a higher adsorption coefficient than alkenes, thus preventing an over-reduction to alkanes. This also explains the improved selectivity with phosphine ligands, but also other ligands, such as carbenes. With the previous results in hand, the same group investigated silica-supported copper nanoparticles additionally modified with NHC ligands for the *Z*-selective semi-hydrogenation of alkynes.<sup>[110]</sup> Again, high selectivities and full conversion of alkynes was achieved.

In addition to copper catalysts that utilize gaseous H<sub>2</sub>, numerous examples for transfer semi-hydrogenations have been reported. One early report from 2014 focused on the conversion of terminal aryl- and alkyl-alkynes with phosphinic

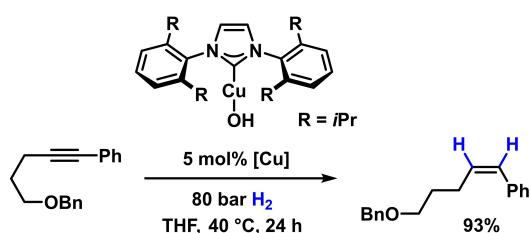
acid in the presence of copper(II) citrate and catalytic amounts of urotropine, which inhibits the homocoupling of the terminal alkynes (Scheme 44).<sup>[111]</sup> Functional groups such as ethers, halides, esters, carboxylic acids, and internal alkenes and alkynes were tolerated under the reaction conditions. Mechanistic proposals involve the initial reduction of the copper(II) species to a copper(I) hydride. After coordination of the alkyne, a copper vinyl complex is formed after *cis*-hydrometallation, which is then protonated and reduced by phosphinic acid. A potential side reaction involves the (reversible) formation of a copper alkynyl species, which was proven by deuteration experiments – all H atoms in the terminal alkene were nearly fully deuterated, which necessitates the prior deuteration of the terminal alkyne under the reaction conditions. A wide variety of copper-catalyzed transfer semi-hydrogenation systems employ the silane derivative polymethylhydrosiloxane (PMHS) as the



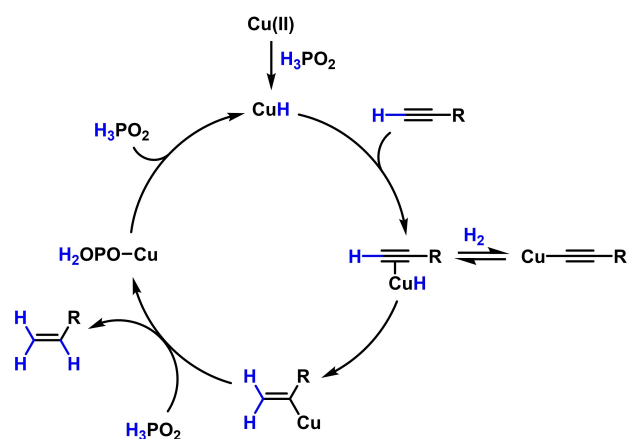
**Scheme 41.** Proposed mechanism of the Cu-catalyzed Z-selective semi-hydrogenation of internal alkynes involving a copper(I) hydride species and an alcohol as the sources of hydrogen.<sup>[105]</sup>



**Scheme 42.** A heterolytic hydrogen bond cleavage with a tethered copper(I) alkoxide complex.<sup>[106]</sup>



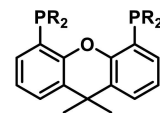
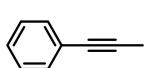
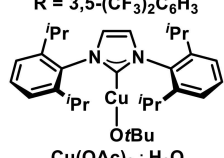
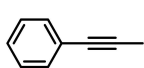
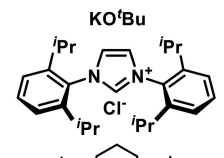
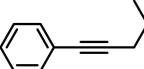
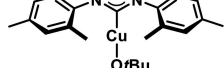
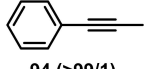
**Scheme 43.** IPrCuOH-catalyzed semi hydrogenation of internal alkynes.<sup>[107]</sup>



**Scheme 44.** Mechanistic proposal for the copper-catalyzed transfer semi-hydrogenation of terminal alkynes using phosphinic acid  $\text{H}_3\text{PO}_2$ .<sup>[111]</sup>

hydride source and an alcohol (mostly  $t\text{BuOH}$ ) as the proton source.<sup>[112]</sup> Examples with their respective copper catalyst, ligand, and reaction conditions are given in Table 6 with the appropriate literature reference. A special case of silane-mediated semi-hydrogenations has been reported by Duan et al., who developed a protocol for the conversion of alkynyl amides to Z-configured  $\alpha,\beta$ -unsaturated amides.<sup>[113]</sup> Specifically, an excess of  $\text{Me}(\text{EtO})_2\text{SiH}$  is used in combination with 10 mol% of  $\text{CuCl}_2$  and dppe in the presence of excess LiOMe in THF. At room temperature, a multitude of (hetero)aryl-substituted alkynyl amides is converted to the (Z)-alkene within 8 h in good to excellent yields. Unfortunately, the authors did not report the amount of (E)- $\alpha,\beta$ -unsaturated amide formed. Similar to such silane-based protocols, a Z-selective system based on an alcohol and boron was reported by Bao et al. in 2019.<sup>[114]</sup> *In situ* formed  $\text{IMes-Cu-}t\text{-butoxide}$  was combined with bis(pinacolato)diboron and ethanol to form a copper(I) hydride intermediate, which then further reacts with the alkyne at room temperature within 5 h in a similar fashion to the mechanisms described earlier in this review. Similarly, an alternative  $\text{B}_2\text{pin}_2$ -mediated approach was presented in a recent report by Huang and co-workers.<sup>[115]</sup> The Cu catalyst is formed *in situ* by the action of 4,4'-bipyridine on  $\text{Cu}(\text{OAc})_2 \cdot 2\text{H}_2\text{O}$ . Contrary to Bao et al.,<sup>[114]</sup> only a sub-stoichiometric amount of  $\text{KO}^t\text{Bu}$  (0.3 equiv.) is required and methanol is used as the hydrogen source as

**Table 6.** Cu-catalyzed transfer semi-hydrogenations of alkynes using combinations of silane/alcohol as formal hydrogen sources.<sup>[112]</sup>

Entry	Cu/L catalyst	Conditions	Alkyne	Yield alkenes [%] (Z/E)
		$\text{R}^1\text{C}\equiv\text{CR}^2 \xrightarrow[\text{Solvent, T, t}]{[\text{Cu}], \text{L}} \begin{matrix} \text{H} & \text{H} \\   &   \\ \text{R}^1 & \text{R}^2 \end{matrix} + \begin{matrix} \text{H} & \text{R}^2 \\   &   \\ \text{R}^1 & \text{H} \end{matrix}$		
			<i>major</i>	<i>minor</i>
1 <sup>[112a]</sup>	$\text{Cu}(\text{OAc})_2 \cdot \text{H}_2\text{O}$ 	2 mol% [Cu] $\text{C}_6\text{H}_{14}/\text{THF}$ 1:1 r.t.–65 °C, 20 h		<b>98 (&gt;99/1)</b>
2 <sup>[112b,c]</sup>	$\text{Cu}(\text{OAc})_2 \cdot \text{H}_2\text{O}$ 	2 mol% [Cu] PhMe 45 °C, 8 h		<b>98 (&gt;99/1)</b>
3 <sup>[112d]</sup>	$\text{KO}^t\text{Bu}$ 	5 mol% [Cu] PhMe r.t. –50 °C, 3–30 h		<b>89 (&gt;99/1)</b>
4 <sup>[112e]</sup>	$\text{Cu}(\text{OAc})_2 \cdot \text{H}_2\text{O}$ 	5 mol% [Cu] $\text{C}_6\text{D}_6$ r.t. –65 °C, 2 h		<b>94 (&gt;99/1)</b>

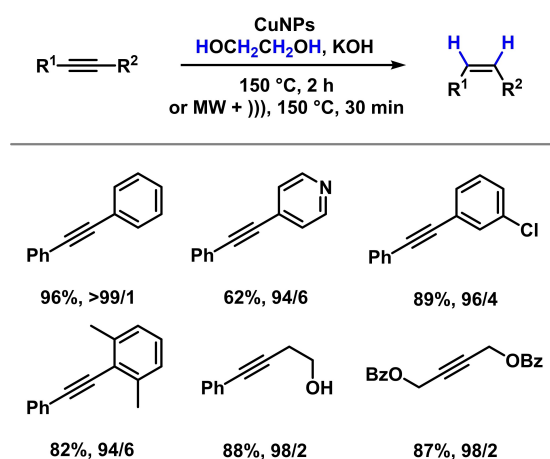
[a] PMHS = polymethylhydrosiloxane.

opposed to ethanol, but higher temperature (60 °C) and longer reactions times (18 h) were required.

With the air-stable [CuOH(IPr)] catalyst developed by the Teichert group, ammonia-borane has been used as hydrogen source for a Z-selective transfer-hydrogenation.<sup>[116]</sup> No additional bases or alcohols were required. Additionally, this protocol was successfully applied in the hydrogenation of  $\alpha,\beta$ -unsaturated esters. With the ambition to entirely avoid the production of stoichiometric amounts of Si- or B-containing waste, a transfer semi-hydrogenation protocol with an alcohol as the sole hydride and proton source was reported in 2019 by Teichert and co-workers.<sup>[117]</sup> [CuCl(SiMes)] with stoichiometric amounts of NaOBu in <sup>t</sup>PrOH enabled Z-selective semi-hydrogenations of internal alkynes at 140 °C and prolonged reaction times (24 h).

In 2021, Moran and co-workers described the Z-selective semi-hydrogenation of internal alkynes catalyzed by copper nanoparticles, using ethylene glycol as the hydrogen source in the presence of an excess of KOH (Scheme 45).<sup>[118]</sup> The Cu-NPs were previously prepared by the reduction of CuSO<sub>4</sub> with NaBH<sub>4</sub> in a basic water/ethylene glycol mixture. A variety of aryl- and alkyl-substituted alkynes bearing functional groups such as amines, ketones or halides were hydrogenated to the respective (Z)-alkene with good to excellent yields and selectivities. Alkanes were not observed. Elevated temperatures (150 °C) are necessary, however, the authors achieved reduction of reaction time from 2 h with conventional heating to 30 min under combined microwave and ultrasound irradiation.

Park et al. presented an alternative Z-selective copper nanoparticle approach, using 10 mol% copper(II) sulfate and 3 equiv. ammonia-borane in ethanol to generate the CuNPs under the reaction conditions.<sup>[119]</sup> This user-friendly protocol delivers excellent yields and Z-selectivities after 3 h at 40 °C, while tolerating critical functional groups such as amines, alcohols or heteroarenes. Both internal and terminal as well as aryl- and alkyl-substituted alkynes are successfully semi-hydrogenated.



**Scheme 45.** Scope of the Z-selective semi-hydrogenation of internal alkynes using Cu nanoparticles and ethylene glycol as hydrogen source. Isolated yields and Z/E ratios for conventional heating below each substrate. Yields and selectivities are similar with combined microwave and ultrasound radiation.<sup>[118]</sup>

Usually, yields and Z-selectivities >90% were achieved, albeit with trace amounts of alkane occasionally being detected. At the same time, Kusy and Grela presented a similar approach, using CuCl<sub>2</sub>·2H<sub>2</sub>O instead to generate the CuNPs *in situ* using ammonia-borane in a water/THF mixture.<sup>[120]</sup> This approach gave similarly satisfactory results as the system by Park et al. Though with slightly higher temperatures (60 °C) and reaction times of up to 24 h, the authors achieved a lower catalyst loading (2 mol%) with a lower excess of H<sub>3</sub>N-BH<sub>3</sub> (2 equiv.) and presented a larger, more diverse substrate scope, additionally including halides, esters and acetals.

An innovative photochemical approach using a Cu@TiO<sub>2</sub> catalyst has been reported by Kominami et al., which enabled a Z-selective transfer-hydrogenation of internal alkynes at room temperature under UV irradiation.<sup>[121]</sup> <sup>t</sup>PrOH served as the hydrogen source.

## 11. Zinc<sup>[122,123]</sup>

Besides examples where Zn merely acts as a solid support for other metal catalysts (e.g. iron nanoparticles immobilized on ZnO),<sup>[50]</sup> there is only a single report with zinc being directly involved as co-catalyst.<sup>[124]</sup> The reduction of [PdCl<sub>2</sub>(PPh<sub>3</sub>)<sub>2</sub>] with zinc metal in the presence of ZnI<sub>2</sub> afforded a catalytic system capable of an E-selective semi-hydrogenation of internal alkynes. Potential mechanistic ideas involve an initial Z-selective hydrogenation step (heterogeneous catalyst) and a subsequent Z/E-isomerization (likely a homogeneous process). It was postulated that ZnI<sub>2</sub> facilitates the reduction of *in situ* formed [PdI<sub>2</sub>(PPh<sub>3</sub>)<sub>2</sub>] to heterogeneous Pd species and that ZnI<sub>2</sub> increases the E-selectivity. Additionally, ZnI<sub>2</sub> seems to reduce the amount of alkene over-hydrogenation and therefore improves the chemoselectivity of the overall process.

## 12. Summary and conclusions

For the early transition metals (scandium, titanium, vanadium, and chromium) as well as zinc only few examples for selective alkyne semi-hydrogenations have thus far been reported. Manganese, iron, cobalt, nickel, and copper, on the other hand, were intensely investigated in the past decade. Given the multitude of astonishing breakthroughs and the sustainability of 3d metals, a decline in research interest is highly unlikely.

Various heterogenous systems based on nanoparticle catalysis as well as homogenous systems were explored in this review. Heterogenous catalysis is dominated by Z-selectivity, while homogenous catalysis may lead to both Z- and E-isomers. In the latter case, the (E)-alkene is typically formed via a *cis*-hydrogenation/isomerization sequence featuring a (Z)-alkene intermediate. Several reports of homogenous catalysts bearing multidentate pincer ligands were presented. Their high popularity stems from their ability to effectively prevent the often highly reduced metals from agglomerating while still offering open coordination sites for the alkyne and hydrogen.

With Brown's discovery of P-2 Nickel in 1963,<sup>[77]</sup> it quickly rose to fame to become the most common non-noble-metal approach to alkyne semi-hydrogenation in synthetic applications, which is still in use today.<sup>[78-81]</sup> Since then, substantial progress has been made in the field of nickel-catalyzed semi-hydrogenations in terms of yields, stereoselectivities, chemoselectivities and sustainability. Noteworthy examples of the publications explored in this review, without any claim to completeness, include the Ni-fructose@SiO<sub>2</sub> catalyst by Beller et al. that enabled very high yields, stereoselectivities, and chemoselectivities (Scheme 36).<sup>[94]</sup> At 10 bar H<sub>2</sub> pressure and 100 °C in a high-pressure reactor, the conditions tolerated halides, anhydrides, and aldehyde functions and continuously gave >99% Z-selectivities. However, preparation of the catalyst requires high-temperature pyrolysis under conditions that may be out of reach for many laboratories. Another catalyst type that exhibited high levels of activity and selectivity is the solid-supported Ni<sub>3</sub>N nanorods by Shi and co-workers (Table 4).<sup>[98]</sup> Chemoselective reactions proceeded in the presence of aryl bromides, nitriles, esters, alcohols and ketones. However, elevated pressures of H<sub>2</sub> (20 bar) were required. The nanorods need be prepared by pyrolysis of nickel(II) nitrate under precise conditions, which required an additional working step and proper equipment.

In contrast to its neighbor in the periodic table, Cu catalysts have only recently been discovered as semi-hydrogenation catalysts with good levels of activity and stereocontrol under mild conditions. Examples include the use of copper nanoparticles generated by reduction of CuSO<sub>4</sub> using NaBH<sub>4</sub> by Moran and co-workers,<sup>[119]</sup> bearing close resemblance to P-2 Ni. The complete absence of dihydrogen or sophisticated hydrogen sources makes this protocol, employing available ethylene glycol as the H<sub>2</sub> source, easily accessible and sustainable. Excellent functional group tolerance towards ketones, aryl chlorides, free amines and N-heterocycles significantly expand the possible substrate palette.

The use of a hydrido manganese complex by the Kirchner group<sup>[39]</sup> (Scheme 13, Table 2) is a rare, remarkable example of an E-selective semi-hydrogenation. High yields, selectivities and functional group tolerance paired with low-cost reagents and relatively mild conditions makes for an operationally simple protocol. However, inconveniently, the pre-catalyst must be synthesized in multiple steps. Another striking example stems from the cobalt realm: The system developed by Li and co-workers<sup>[70]</sup> (Scheme 25) features switchable stereoselectivity directed merely by the presence or absence of the phosphine ligand. The mild conditions tolerate various vulnerable functions such as halides, nitriles and esters, as well as free alcohols and amines. Moreover, water is used as the sole hydrogen source.

The direct use of water under either reductive or electrolytic conditions as opposed to using pre-produced (green) hydrogen is a strong candidate for future-proof protocols with further improvement in sustainability and efficiency. In this regard, the recent resurgence of electrochemical synthesis has enabled innovative protocols of stereoselective alkyne hydrogenations.<sup>[95,96]</sup> The ability to fine-tune the elemental steps

of single-electron transfer and protonation by independent variations of electrode materials, electrolytes, conditions, metal-ligand complexes, and Brønsted acids gives rise to an enormous optimization potential. We firmly believe that electrochemical hydrogenation protocols will receive substantial research interest in the near future.

Overall, a range of problems and drawbacks of 3d-metal-catalyzed semi-hydrogenation pose challenges which must be overcome before mainstream use is conceivable. Several (reduced) 3d metal complexes are highly susceptible to water and oxygen, requiring inert conditions with rigorous exclusion of both. Moreover, their significant oxophilicity and general vulnerability to coordinating atoms lead to functional group tolerances and chemoselectivities that are often poor to mediocre. Particularly functions that are easily reduced, such as halides, ketones, aldehydes, esters, nitriles, or acidic substrates with alcohols or carboxylic acids frequently lead to poor yields.

However, enormous progress has been made in the past years, with significantly milder reaction conditions having been achieved. From the frequently reported harsh conditions (> 50 bar H<sub>2</sub>, > 100 °C, long reaction times), high catalyst loadings, laborious catalyst preparation and low yields and selectivities in early publications, remarkable improvements in all areas have been accomplished. A plethora of new reports now demonstrate ambient conditions with atmospheric hydrogen pressure or transfer hydrogenation reagents, permitting a broader application with a simpler reaction set-up. This allows for several user-friendly protocols using commercially available precursors under accessible conditions which might threaten to dethrone the Lindlar catalyst as the method of choice for alkyne semi-hydrogenation in the foreseeable future.

## Acknowledgements

*This work was supported by the Priority Research Program SPP 1708 of the Deutsche Forschungsgemeinschaft (DFG) and the European Research Council (ERC, CoG 683150 to A.J.v.W.). M.-O.W.S.S. is a fast track doctoral fellow of the Hamburg Research Academy at the University of Hamburg. Open Access funding enabled and organized by Projekt DEAL.*

## Conflict of Interest

The authors declare no conflict of interest.

## Data Availability Statement

Data sharing is not applicable to this article as no new data were created or analyzed in this study.

**Keywords:** alkenes · alkynes · semi-hydrogenation · stereoselectivity · transition metals · hydrogen

- [1] J. Humphreys, R. Lan, S. Tao, *Adv. Energy Sustainability Res.* **2021**, *2*, 2000043.
- [2] M. T. Tarrago-Trani, K. M. Phillips, L. E. Lemar, J. M. Holden, *J. Acad. Nutr. Diet.* **2006**, *106*, 867–880.
- [3] a) G. A. Olah, *Angew. Chem. Int. Ed.* **2005**, *44*, 2636–2639; b) G. A. Olah, A. Goeppert, G. K. S. Prakash, *J. Org. Chem.* **2009**, *74*, 487–498.
- [4] a) G. L. Parker, L. K. Smith, I. R. Baxendale, *Tetrahedron* **2016**, *72*, 1645–1652; b) E. Breitmeier, *Terpene. Aromen, Düfte, Pharmaka, Pheromone*, Wiley-VCH, Weinheim, **2005**; c) W.-Y. Siau, Y. Zhang, Y. Zhao, *Top. Curr. Chem.* **2012**, *327*, 33–58; d) R. H. Grubbs, T. M. Trnka, *Ruthenium in Organic Synthesis* (Ed.: S.-I. Murahashi), Wiley-VCH, Weinheim, **2004**; e) A. Welther, A. Jacobi von Wangelin, *Curr. Org. Chem.* **2013**, *17*, 326–335; f) J. F. Teichert, *Homogeneous Hydrogenation with Non-Precious Catalysts*, Wiley-VCH, Weinheim, **2019**; g) J. G. de Vries, C. J. Elsevier, *Handbook of Homogeneous Hydrogenation*, Wiley-VCH, **2006**; h) C. Oger, V. Butel-Poncé, A. Guy, L. Balas, J.-C. Rossi, T. Durand, J.-M. Galano, *Chem. Eur. J.* **2010**, *16*, 13976–13980.
- [5] For selected examples of selective alkyne semi-hydrogenations in total syntheses of natural products, see: a) J. A. Marshall, M. P. Bourbeau, *J. Org. Chem.* **2002**, *67*, 2751–2754; b) L. E. Overman, A. S. Thompson, *J. Am. Chem. Soc.* **1988**, *110*, 2248–2256; c) B. M. Trost, Z. Shi, *J. Am. Chem. Soc.* **1994**, *116*, 7459–7460; d) R. K. Boeckman Jr., E. W. Thomas, *J. Am. Chem. Soc.* **1977**, *99*, 2805–2806; e) W. H. Pearson, F. E. Lovering, *J. Org. Chem.* **1998**, *63*, 3607–3617; f) A. B. Smith, S. S.-Y. Chen, F. C. Nelson, J. M. Reichert, B. A. Salvatore, *J. Am. Chem. Soc.* **1997**, *119*, 10935–10946; g) P. Yang, M. Yao, J. Li, Y. Li, A. Li, *Angew. Chem. Int. Ed.* **2016**, *55*, 6964–6968; h) K. C. Nicolaou, N. A. Petasis, R. E. Zipkin, *J. Am. Chem. Soc.* **1982**, *104*, 5560–5562; i) T. Maehara, K. Motoyama, T. Toma, S. Yokoshima, T. Fukuyama, *Angew. Chem. Int. Ed.* **2017**, *56*, 1549–1552; j) T. Itoh, N. Yamazaki, C. Kibayashi, *Org. Lett.* **2002**, *4*, 2469–2472; k) R. B. Woodward, M. P. Cava, W. D. Ollis, A. Hunger, H. U. Daeniker, K. Schenker, *J. Am. Chem. Soc.* **1954**, *76*, 4749–4751; l) R. Baker, V. B. Rao, *J. Chem. Soc., Perkin Trans. 1* **1982**, 69–71; m) M. Jacobson, M. Beroza, W. A. Jones, *J. Am. Chem. Soc.* **1961**, *83*, 4819–4824; n) J. E. McMurry, J. Melton, *J. Am. Chem. Soc.* **1971**, *93*, 5309–5311; o) A. Fürstner, G. Seidel, *J. Organomet. Chem.* **2000**, *606*, 75–78; p) A. Fürstner, F. Stelzer, A. Rumbo, H. Krause, *Chem. Eur. J.* **2002**, *8*, 1856–1871.
- [6] a) For a preceding review on alkyne transfer semi-hydrogenations by transition metal catalysis, including 3d metals, see: D. Decker, H.-J. Drexler, D. Heller, T. Beweries, *Catal. Sci. Technol.* **2020**, *10*, 6449–6463; b) For an interesting perspective on selective alkyne semi-hydrogenations in the synthesis of polyfunctionalized molecules, see: C. Oger, L. Balas, T. Durand, J.-M. Galano, *Chem. Rev.* **2013**, *113*, 1313–1350.
- [7] a) H. Lindlar, R. Dubuis, *Org. Synth.* **1966**, *46*, 89–91; b) H. Lindlar, *Helv. Chim. Acta* **1952**, *35*, 446–450; c) W.-Y. Siau, Y. Zhang, Y. Zhao, *Top. Curr. Chem.* **2012**, *327*, 33–58.
- [8] K. C. K. Swamy, A. S. Reddy, K. Sandeep, A. Kalyani, *Tetrahedron Lett.* **2018**, *59*, 419–429.
- [9] a) P. T. Anastas, J. C. Warner In: *Green Chemistry: Theory and Practice*, Oxford University Press, New York, **1998**; b) P. Anastas, N. Eghbali, *Chem. Soc. Rev.* **2010**, *39*, 301–312.
- [10] a) J. J. Stephanos, A. W. Addison In: *Chemistry of Metalloproteins*, John Wiley & Sons Inc, New York, **2014**; b) W. Kaim, B. Schwederski, A. Klein, *Bioinorganic Chemistry: Inorganic Elements in the Chemistry of Life*, 2nd ed., Wiley, New York, **2013**.
- [11] For a comprehensive review on 3d-metal-catalyzed C–B bond formation, including alkyne hydroborations, see: S. K. Bose, L. Mao, L. Kuehn, U. Radius, J. Nekvinda, W. L. Santos, S. A. Westcott, P. G. Steel, T. B. Marder, *Chem. Rev.* **2021**, *121*, 13238–13341.
- [12] For alternative scandium-catalyzed hydroborations of alkynes, see for example: S. Mandal, P. K. Verma, K. Geetharani, *Chem. Commun.* **2018**, *54*, 13690–13693.
- [13] D. S. Levine, T. D. Tilley, R. A. Andersen, *Chem. Commun.* **2017**, *53*, 11881–11884.
- [14] For alternative titanium-catalyzed hydrosilylation of alkynes, see for example: T. Takahashi, F. Bao, G. Gao, M. Ogasawara, *Org. Lett.* **2003**, *5*, 3479–3481.
- [15] For alternative titanium-catalyzed hydroborations of alkynes, see for example: a) X. He, J. F. Hartwig, *J. Am. Chem. Soc.* **1996**, *118*, 1696–1702; b) J. F. Hartwig, C. N. Muhoro, *Organometallics* **2000**, *19*, 30–38; c) J. Bhattacharjee, A. Harinath, K. Bano, T. K. Panda, *ACS Omega* **2020**, *5*, 1595–1606.
- [16] a) K. Sonogashira, N. Hagihara, *Bull. Chem. Soc. Jpn.* **1966**, *39*, 1178–1182; b) B. Demerseman, P. Le Coupanec, P. H. Dixneuf, *J. Organomet. Chem.* **1985**, *287*, 3, C35–C38.
- [17] S. Imai, K. Nakanishi, A. Tanaka, H. Kominami, *ChemCatChem* **2020**, *12*, 1609–1616.
- [18] A. G. Campaña, R. E. Estévez, N. Fuentes, R. Robles, J. M. Cuerva, E. Buñuel, D. Cárdenas, J. E. Oltra, *Org. Lett.* **2007**, *9*, 2195–2198.
- [19] For a comprehensive review on general vanadium catalysis, see: R. R. Langeslay, D. M. Kaphan, C. L. Marshall, P. C. Stair, A. P. Sattelberger, M. Delferro, *Chem. Rev.* **2019**, *119*, 2128–2191.
- [20] H. S. La Pierre, J. Arnold, F. D. Toste, *Angew. Chem. Int. Ed.* **2011**, *50*, 3900–3903.
- [21] S. A. Holmes, D. F. Schafer, P. T. Wolczanski, E. B. Lobkovsky, *J. Am. Chem. Soc.* **2001**, *123*, 10571–10583.
- [22] K. K. Tanabe, M. S. Ferrandon, N. A. Sildake, S. J. Kraft, G. Zhang, J. Niklas, O. G. Poluektov, S. J. Lopykinski, E. E. Bunel, T. R. Krause, J. T. Miller, A. S. Hock, S. T. Nguyen, *Angew. Chem. Int. Ed.* **2014**, *53*, 12055–12058.
- [23] H. Sohn, J. Camacho-Bunquin, R. R. Langeslay, P. A. Ignacio-de Leon, J. Niklas, O. G. Poluektov, C. Liu, J. G. Connell, D. Yang, J. Kropf, H. Kim, P. C. Stair, M. Ferrandon, M. Delferro, *Chem. Commun.* **2017**, *53*, 7325–7328.
- [24] M. Sodeoka, M. Shibasaki, *J. Org. Chem.* **1985**, *50*, 1147–1149.
- [25] J. Camacho-Bunquin, N. A. Sildake, G. Zhang, J. Niklas, O. G. Poluektov, S. T. Miller, J. T. Miller, A. S. Hock, *Organometallics* **2015**, *34*, 947–952.
- [26] B. J. Gregori, M. Nowakowski, A. Schoch, S. Pöllath, J. Zweck, M. Bauer, A. Jacobi von Wangelin, *ChemCatChem* **2020**, *12*, 5359–5363.
- [27] Metal-catalyzed (semi-)hydrogenation of alkynes and nitriles: D. M. Sharma, B. Punji, *Chem. Asian J.* **2020**, *15*, 690–708.
- [28] For a review on manganese-catalyzed transfer hydrogenations, including alkyne semi-hydrogenations, see: K. Azouzi, D. A. Valyaev, S. Bastin, J.-B. Sortais, *Curr. Opin. Green Sustain.* **2021**, *31*, 100511–100517.
- [29] For alternative stereoselective synthesis by manganese-catalyzed hydrosilylation of alkynes, see for example: a) X. Yang, C. Wang, *Angew. Chem. Int. Ed.* **2018**, *57*, 923–928; b) X. Yang, C. Wang, *Chem. Asian J.* **2018**, *13*, 2307–2315; c) H. Liang, Y.-X. Ji, R.-H. Wang, Z.-H. Zhang, B. Zhang, *Org. Lett.* **2019**, *21*, 2750–2754.
- [30] For alternative stereoselective synthesis by Mn-catalyzed hydroboration of alkynes, see for example: A. Brzozowska, V. Zubar, R.-C. Ganardi, M. Rueping, *Org. Lett.* **2020**, *22*, 3765–3769.
- [31] Y. Wang, M. Wang, Y. Li, Q. Liu, *Chem* **2021**, *7*, chempr.2020.11.013.
- [32] Y.-P. Zhou, Z. Mo, M.-P. Luecke, M. Driess, *Chem. Eur. J.* **2018**, *24*, 4780–4784.
- [33] A. Brzozowska, L. M. Azofra, V. Zubar, I. Atodiresei, L. Cavallo, M. Rueping, O. El-Sepelgy, *ACS Catal.* **2018**, *8*, 4103–4109.
- [34] J. Sklyaruk, V. Zubar, J. C. Borghs, M. Rueping, *Org. Lett.* **2020**, *22*, 6067–6071.
- [35] A. Torres-Calis, J. J. García, *Catal. Sci. Technol.* **2022**, *12*, 3004–3015.
- [36] V. Zubar, J. Sklyaruk, A. Brzozowska, M. Rueping, *Org. Lett.* **2020**, *22*, 5423–5428.
- [37] M. Garbe, S. Budweg, V. Papa, Z. Wei, H. Hornke, S. Bachmann, M. Scalone, A. Spannenberg, H. Jiao, K. Junge, M. Beller, *Catal. Sci. Technol.* **2020**, *10*, 3994–4001.
- [38] a) J. R. Khushnutdinova, D. Milstein, *Angew. Chem. Int. Ed.* **2015**, *54*, 12236–12273; b) H. Li, T. P. Gonçalves, D. Lupp, K.-W. Huang, *ACS Catal.* **2019**, *9*, 1619–1629; c) Y. Wang, L. Zhu, Z. Shao, G. Li, Y. Lan, Q. Liu, *J. Am. Chem. Soc.* **2019**, *141*, 17337–17349.
- [39] R. A. Farrar-Tobar, S. Weber, Z. Csendes, A. Ammataro, S. Fleissner, H. Hoffmann, L. F. Veiros, K. Kirchner, *ACS Catal.* **2022**, *12*, 2253–2260.
- [40] For alternative stereoselective synthesis by iron-catalyzed hydrosilylation of alkynes, see for example: a) M. D. Greenhalgh, A. S. Jones, S. P. Thomas, *ChemCatChem* **2015**, *7*, 190–222; b) D. Wei, C. Darcel, *J. Org. Chem.* **2020**, *85*, 14298–14306; c) S. Enthaler, M. Haberberger, E. Irran, *Chem. Asian J.* **2011**, *6*, 1613–1623; d) C. Belger, B. Plietker, *Chem. Commun.* **2012**, *48*, 5419–5421; e) M. D. Greenhalgh, D. J. Frank, S. P. Thomas, *Adv. Synth. Catal.* **2014**, *356*, 584–590; f) C. Johnson, M. Albrecht, *Catal. Sci. Technol.* **2018**, *8*, 2779–2783; g) M.-Y. Hu, P. He, T.-Z. Qiao, W. Sun, W.-T. Li, J. Lian, J.-H. Li, S.-F. Zhu, *J. Am. Chem. Soc.* **2020**, *142*, 16894–16902.
- [41] For alternative stereoselective synthesis by iron-catalyzed hydroboration of alkynes, see for example: a) M. D. Greenhalgh, S. P. Thomas, *Chem. Commun.* **2013**, *49*, 11230–11232; b) M. Haberberger, S. Enthaler, *Chem. Asian J.* **2013**, *8*, 50–54; c) V. S. Rawat, B. Sreedhar, *Synlett* **2014**, *25*, 1132–1136; d) K.-N. T. Tseng, J. W. Kampf, N. K. Szymczak, *ACS Catal.* **2015**, *5*, 411–415; e) M. Espinal-Viguri, C. R. Woof,



- R. L. Webster, *Chem. Eur. J.* **2016**, *22*, 11605–11608; f) K. Nakajima, T. Kato, Y. Nishibayashi, *Org. Lett.* **2017**, *19*, 4324–4326; g) N. Gorgas, L. G. Alves, B. Stöger, A. M. Martins, L. F. Veiros, K. Kirchner, *J. Am. Chem. Soc.* **2017**, *139*, 8130–8133; h) N. Gorgas, B. Stöger, L. F. Veiros, K. Kirchner, *ACS Catal.* **2018**, *8*, 7973–7982; i) S. Garhwal, N. Fridman, G. de Ruiter, *Inorg. Chem.* **2020**, *59*, 13817–13821; j) F. Rami, F. Bächtle, B. Plietker, *Catal. Sci. Technol.* **2020**, *10*, 1492–1497; k) A. Singh, S. Shafiei-Haghighi, C. R. Smith, D. K. Unruh, M. Findlater, *Asian J. Org. Chem.* **2020**, *9*, 416–420; l) X.-F. Duan, *Chem. Commun.* **2020**, *56*, 14937–14961.
- [42] a) A. F. Thompson Jr., S. B. Wyatt, *J. Am. Chem. Soc.* **1940**, *62*, 2555–2556; b) A. F. Thompson Jr., E. N. Shaw, *J. Am. Chem. Soc.* **1942**, *64*, 363–366.
- [43] a) S.-I. Taira, *Bull. Chem. Soc. Jpn.* **1962**, *35*, 840–844; b) K. Hata, I. Motoyama, K. Sakai, *Org. Prep. Proc. Int.* **1972**, *4*, 179–209.
- [44] M. Armbrüster, K. Kovnir, M. Friedrich, D. Teschner, G. Wowsnick, M. Hahne, P. Gille, L. Szentmiklósi, M. Feuerbacher, M. Heggen, F. Girgsdies, D. Rosenthal, R. Schlögl, Y. Grin, *Nature Mater.* **2012**, *11*, 690–693.
- [45] C. U. Pittman Jr., R. C. Ryan, J. McGee, J. P. O'Connor, *J. Organomet. Chem.* **1979**, *178*, C43–C49.
- [46] a) C. Bianchini, A. Mell, M. Peruzzini, F. Vizza, F. Zanobini, *Organometallics* **1989**, *8*, 2080–2082; b) C. Bianchini, A. Mell, M. Peruzzini, P. Frediani, C. Bohanna, M. A. Esteruelas, L. A. Oro, *Organometallics* **1992**, *11*, 138–145.
- [47] G. Wienhöfer, F. A. Westerhaus, R. V. Jagadeesh, K. Junge, H. Junge, M. Beller, *Chem. Commun.* **2012**, *48*, 4827–4829.
- [48] S. C. Bart, E. Lobkovsky, P. J. Chirik, *J. Am. Chem. Soc.* **2004**, *126*, 13794–13807.
- [49] T. N. Gieshoff, M. Villa, A. Welther, M. Plois, U. Chakraborty, R. Wolf, A. Jacobi von Wangelin, *Green Chem.* **2015**, *17*, 1408–1413.
- [50] T. N. Gieshoff, A. Welther, M. T. Kessler, M. H. G. Precht, A. Jacobi von Wangelin, *Chem. Commun.* **2014**, *50*, 2261–2264.
- [51] B. J. Gregori, F. Schwarzhuber, S. Pöllath, J. Zweck, L. Fritsch, R. Schoch, M. Bauer, A. Jacobi von Wangelin, *ChemSusChem* **2019**, *12*, 3864–3870.
- [52] T. N. Gieshoff, U. Chakraborty, M. Villa, A. Jacobi von Wangelin, *Angew. Chem. Int. Ed.* **2017**, *56*, 3585–3589.
- [53] M. Tejada-Serrano, J. R. Cabrero-Antonino, V. Mainar-Ruiz, M. López-Haro, J. C. Hernández-Garrido, J. J. Calvino, A. Leyva-Pérez, A. Corma, *ACS Catal.* **2017**, *7*, 3721–3729.
- [54] N. Gorgas, J. Brüning, B. Stöger, S. Vanicek, M. Tilset, L. F. Veiros, K. Kirchner, *J. Am. Chem. Soc.* **2019**, *141*, 17452–17458.
- [55] D. Srimani, Y. Diskin-Posner, Y. Ben-David, D. Milstein, *Angew. Chem. Int. Ed.* **2013**, *52*, 14131–14134.
- [56] M. K. Karunananda, N. P. Mankad, *J. Am. Chem. Soc.* **2015**, *137*, 14598–14601.
- [57] M. Espinal-Viguri, S. E. Neale, N. T. Coles, S. A. Macgregor, R. L. Webster, *J. Am. Chem. Soc.* **2019**, *141*, 572–582.
- [58] a) P.-H. Phua, L. Lefort, J. A. F. Boogers, M. Tristany, J. G. de Vries, *Chem. Commun.* **2009**, *25*, 3747–3749; b) C. Rangheard, C. d. J. Fernández, P.-H. Phua, J. Hoorn, L. Lefort, J. G. de Vries, *Dalton Trans.* **2010**, *39*, 8464–8471; c) V. Kelsen, B. Wendt, S. Werkmeister, K. Junge, M. Beller, B. Chaudret, *Chem. Commun.* **2013**, *49*, 3416–3418; d) M. Stein, J. Wieland, P. Steurer, F. Tölle, R. Mülhaupt, B. Breit, *Adv. Synth. Catal.* **2011**, *353*, 523–527.
- [59] For alternative stereoselective synthesis by cobalt-catalyzed hydro-silylation of alkynes, see for example: a) M. Isobe, R. Nishizawa, T. Nishikawa, K. Yoza, *Tetrahedron Lett.* **1999**, *40*, 6927–6932; b) S. Tojo, M. Isobe, *Tetrahedron Lett.* **2005**, *46*, 381–384; c) L. Yong, K. Kirleis, H. Butenschön, *Adv. Synth. Catal.* **2006**, *348*, 833–836; d) T. Konno, K.-I. Taku, S. Yamada, K. Moriyasu, T. Ishihara, *Org. Biomol. Chem.* **2009**, *7*, 1167–1170; e) K.-H. Huang, M. Isobe, *Eur. J. Org. Chem.* **2014**, *22*, 4733–4740; f) Z. Mo, J. Xiao, Y. Gao, L. Deng, *J. Am. Chem. Soc.* **2014**, *136*, 17414–17417; g) A. Rivera-Hernández, B. J. Fallon, S. Ventra, C. Simon, M.-H. Tremblay, G. Gontard, E. Derat, M. Amatore, C. Aubert, M. Petit, *Org. Lett.* **2016**, *18*, 4242–4245; h) J. Guo, Z. Lu, *Angew. Chem. Int. Ed.* **2016**, *55*, 10835–10838; i) Z. Zuo, J. Yang, Z. Huang, *Angew. Chem. Int. Ed.* **2016**, *55*, 10839–10843; j) W. J. Tao, C. Wang, Y. W. Tan, S. Ge, *Angew. Chem. Int. Ed.* **2017**, *56*, 4328–4332; k) X. Du, W. Hou, Y. Zhang, Z. Huang, *Org. Chem. Front.* **2017**, *4*, 1517–1521; l) C. Wu, W. J. Teo, S. Ge, *ACS Catal.* **2018**, *8*, 5896–5900; m) G. Wu, U. Chakraborty, A. Jacobi von Wangelin, *Chem. Commun.* **2018**, *54*, 12322–12325; n) H. Wen, X. Wan, Z. Huang, *Angew. Chem. Int. Ed.* **2018**, *57*, 6319–6323; o) D. Kong, B. Hu, M. Yang, D. Chen, H. Xia, *Organometallics* **2019**, *38*, 4341–4350; p) D. Kong, B. Hu, D. Chen, *Chem. Asian J.* **2019**, *14*, 2694–2703; q) H. L. Sang, Y. Hu, S. Ge, *Org. Lett.* **2019**, *21*, 5234–5237; r) Z. Zong, Q. Yu, N. Sun, B. Hu, Z. Shen, X. Hu, L. Jin, *Org. Lett.* **2019**, *21*, 5767–5772; s) C. K. Blasius, H. Wadepohl, L. H. Gade, *Eur. J. Inorg. Chem.* **2020**, *24*, 2335–2342; t) D. Kong, B. Hu, M. Yang, H. Xia, D. Chen, *Organometallics* **2020**, *39*, 4437–4443; u) M. Skrodzki, V. Patroniak, P. Pawluć, *Org. Lett.* **2021**, *23*, 663–667; v) Y. B. Kim, D. Kim, S. U. Dighe, S. Chang, J.-W. Park, *ACS Catal.* **2021**, *11*, 1548–1553; w) J. Sun, L. Deng, *ACS Catal.* **2016**, *6*, 290–300; x) W. Ai, R. Zhong, X. Liu, Q. Liu, *Chem. Rev.* **2019**, *119*, 2876–2953.
- [60] For alternative stereoselective synthesis by cobalt-catalyzed hydro-boration of alkynes, see for example: a) J. V. Obligacion, J. M. Neely, A. N. Yazdani, I. Pappas, P. J. Chirik, *J. Am. Chem. Soc.* **2015**, *137*, 5855–5858; b) H. Ben-Daat, C. L. Rock, M. Flores, T. L. Groy, A. C. Bowman, R. J. Trovitch, *Chem. Commun.* **2017**, *53*, 7333–7336; c) T. Xi, Z. Lu, *ACS Catal.* **2017**, *7*, 1181–1185; d) L. Qiao, L. Zhang, G. Liu, Z. Huang, *Tetrahedron* **2019**, *75*, 4138–4142; e) G. Zhang, S. Li, J. Wu, H. Zeng, Z. Mo, K. Davis, S. Zheng, *Org. Chem. Front.* **2019**, *6*, 3228–3233; f) H. L. Sang, C. Wu, G. G. D. Phua, S. Ge, *ACS Catal.* **2019**, *9*, 10109–10114; g) C. K. Blasius, V. Vasilenko, R. Matveeva, H. Wadepohl, L. H. Gade, *Angew. Chem. Int. Ed.* **2020**, *59*, 23010–23014; h) J. Chen, X. Shen, Z. Lu, *Angew. Chem. Int. Ed.* **2021**, *60*, 690–694.
- [61] G. F. Pregaglia, A. Andreetta, G. F. Ferrari, *J. Organomet. Chem.* **1971**, *30*, 387–405.
- [62] K. Tokmic, A. R. Fout, *J. Am. Chem. Soc.* **2016**, *138*, 13700–13705.
- [63] a) S. Fu, N.-Y. Chen, X. Liu, Z. Shao, S.-P. Luo, Q. Liu, *J. Am. Chem. Soc.* **2016**, *138*, 8588–8594; b) X. Qi, X. Liu, L.-B. Qu, Q. Liu, Y. Lan, *J. Catal.* **2018**, *362*, 25–34.
- [64] K. M. Gramigna, D. A. Dickie, B. M. Foxman, C. M. Thomas, *ACS Catal.* **2019**, *9*, 3153–3164.
- [65] C. Chen, Y. Huang, Z. Zhang, X.-Q. Dong, X. Zhang, *Chem. Commun.* **2017**, *53*, 4612–4615.
- [66] V. G. Landge, J. Pitchaimani, S. P. Midya, M. Subaramanian, V. Madhu, E. Balaraman, *Catal. Sci. Technol.* **2018**, *8*, 428–433.
- [67] B. Raya, S. Biswas, T. V. RajanBabu, *ACS Catal.* **2016**, *6*, 6318–6323.
- [68] F. Chen, C. Kreyenschulte, J. Radnik, H. Lund, A.-E. Surkus, K. Junge, M. Beller, *ACS Catal.* **2017**, *7*, 1526–1532.
- [69] G. Jaiswal, V. G. Landge, M. Subaramanian, R. G. Kadam, R. Zbořil, M. B. Gawande, E. Balaraman, *ACS Sustain. Chem. Eng.* **2020**, *8*, 11058–11068.
- [70] K. Li, R. Khan, X. Zhang, Y. Gao, Y. Zhou, H. Tan, J. Chen, B. Fan, *Chem. Commun.* **2019**, *55*, 5663–5666.
- [71] L. Schmolke, B. J. Gregori, B. Giesen, A. Schmitz, J. Barthel, L. Staiger, R. A. Fischer, A. Jacobi von Wangelin, C. Janiak, *New J. Chem.* **2019**, *43*, 16583–16594.
- [72] A. Sodreau, A. Vivien, A. Moisset, C. Salzemann, C. Petit, M. Petit, *Inorg. Chem.* **2020**, *59*, 13972–13978.
- [73] W.-F. Tian, Y.-Q. He, X.-R. Song, H.-X. Ding, J. Ye, W.-J. Guo, Q. Xiao, *Adv. Synth. Catal.* **2020**, *362*, 1032–1038.
- [74] J. Chen, M. Chu, F. Lyu, J. Gong, L. Wu, L. Liu, Y. Xu, Q. Zhang, *Ind. Eng. Chem. Res.* **2019**, *58*, 21413–21418.
- [75] For alternative stereoselective synthesis by nickel-catalyzed hydro-silylation of alkynes, see for example: a) A. Tillack, S. Pulst, W. Baumann, H. Baudisch, K. Kortus, U. Rosenthal, *J. Organomet. Chem.* **1997**, *532*, 117–123; b) M. R. Chaulagain, G. M. Mahandru, J. Montgomery, *Tetrahedron* **2006**, *62*, 7560–7566; c) J. Berding, J. A. van Paridon, V. H. S. van Rixel, E. Bouwman, *Eur. J. Inorg. Chem.* **2011**, *15*, 2450–2458; d) H. Wang, Y. Huang, X. Wang, X. Cui, F. Shi, *Org. Biomol. Chem.* **2020**, *18*, 7554–7558.
- [76] For alternative stereoselective synthesis by nickel-catalyzed hydro-boration of alkynes, see for example: G. W. Kabalka, C. Narayana, N. K. Reddy, *Synth. Commun.* **1994**, *24*, 1019–1023.
- [77] a) H. C. Brown, C. A. Brown, *J. Am. Chem. Soc.* **1963**, *85*, 1005–1006; b) C. A. Brown, V. K. Ahuja, *J. Chem. Soc., Chem. Commun.* **1973**, 553–554.
- [78] T. V. Hansen, Y. Stenstrøm, *Tetrahedron Asymm.* **2001**, *12*, 1407–1409.
- [79] D. W. Klosowski, S. F. Martin, *Org. Lett.* **2018**, *20*, 1269–1271.
- [80] K. G. Primdahl, M. Aursnes, M. E. Walker, R. A. Colas, C. N. Serhan, J. Dalli, T. V. Hansen, A. Vik, *J. Nat. Prod.* **2016**, *79*, 2693–2702.
- [81] For additional selected examples of P–2-Ni-catalyzed alkyne semi-hydrogenations in syntheses of natural products and pharmaceutically relevant substances, see: a) C. F. Heinrich, E. Widemann, J. Sanz, R. Lugan, T. Heitz, F. Pinot, M. Miesch, L. Miesch, *Eur. J. Org. Chem.* **2015**, *5*, 1130–1136; b) K. C. Nicolaou, K. K. Pulukuri, R. Yu, S. Rigol, P. Heretsch, C. I. Grove, C. R. H. Hale, A. ElMarrouni, *Chem. Eur. J.* **2016**, *22*, 8559–8570; c) R. W. Bates, L. Li, K. Palani, W. Phetsang, J. K. Loh, *Asian J. Org. Chem.* **2014**, *3*, 792–796; d) C.-W. Chien, C. Shi, C. F. Lin, I. Ojima,

- Tetrahedron* **2011**, *67*, 6513–6523; e) O. Dasse, A. Mahadevan, L. Han, B. R. Martin, V. Di Marzo, R. K. Razdan, *Tetrahedron* **2000**, *56*, 9195–9202; f) D. Bland, G. Chambournier, V. Dragan, D. J. Hart, *Tetrahedron* **1999**, *55*, 8953–8966; g) L. Han, R. K. Razdan, *Tetrahedron Lett.* **1998**, *39*, 771–774; h) T. K. M. Shing, K. H. Gibson, J. R. Wiley, C. I. F. Watt, *Tetrahedron Lett.* **1994**, *35*, 1067–1070; i) T. E. Bellas, R. G. Brownlee, R. M. Silverstein, *Tetrahedron* **1969**, *25*, 5149–5153; j) G. Just, B. O'Connor, *Tetrahedron Lett.* **1988**, *29*, 753–756; k) Y.-S. Cheng, W. Yu, Y. Xu, R. G. Salomon, *J. Nat. Prod.* **2017**, *80*, 488–498; l) K. C. Nicolau, K. K. Pulukuri, S. Rigol, P. Heretsch, R. Yu, C. I. Grove, C. R. H. Hale, A. ElMarrouni, V. Fetz, M. Brönstrup, M. Aujay, J. Sandoval, J. Gavriluk, *J. Am. Chem. Soc.* **2016**, *138*, 6550–6560; m) S. P. Chavan, R. K. Kharul, S. K. Kamat, U. R. Kalkote, R. R. Kale, *Synth. Commun.* **2005**, *35*, 987–994; n) K. Lorber, P. Schieberle, A. Buettner, *J. Agric. Food Chem.* **2014**, *62*, 1025–1031; o) R. W. Bates, K. Palani, *Tetrahedron Lett.* **2008**, *49*, 2832–2834; p) R. Mahrwald, H. Schick, K. K. Pivnitsky, S. Schwarz, *J. Prakt. Chem.* **1990**, *332*, 403–413; q) J. M. E. Hughes, J. L. Gleason, *Tetrahedron* **2018**, *74*, 759–768; r) J. T. Feutrill, M. J. Lilly, J. M. White, M. A. Rizzacasa, *Tetrahedron* **2008**, *64*, 4880–4895.
- [82] X. Wen, X. Shi, X. Qiao, Z. Wu, G. Bai, *Chem. Commun.* **2017**, *53*, 5372–5375.
- [83] D. J. Hale, M. J. Ferguson, L. Turculet, *ACS Catal.* **2022**, *12*, 146–155.
- [84] F. Alonso, I. Osante, M. Yus, *Adv. Synth. Catal.* **2006**, *348*, 305–308.
- [85] R. Barrios-Francisco, J. J. García, *Inorg. Chem.* **2009**, *48*, 386–393.
- [86] A. Reyes-Sánchez, F. Cañavera-Buelvas, O. L. Cifuentes-Vaca, M. Flores-Alamo, J. J. García, *Organometallics* **2011**, *30*, 3340–3345.
- [87] T. Chen, J. Xiao, Y. Zhou, S. Yin, L.-B. Han, *J. Organomet. Chem.* **2014**, *749*, 51–54.
- [88] E. Richmond, J. Moran, *J. Org. Chem.* **2015**, *80*, 6922–6929.
- [89] K. Li, C. Yang, J. Chen, C. Pan, R. Fan, Y. Zhou, Y. Luo, D. Yang, B. Fan, *Asian J. Org. Chem.* **2021**, *10*, 2143–2146.
- [90] K. Murugesan, C. B. Bheeter, P. R. Linnebank, A. Spannenberg, J. N. H. Reek, R. V. Jagadeesh, M. Beller, *ChemSusChem* **2019**, *12*, 3363–3369.
- [91] N. O. Thiel, B. Kaewmee, T. T. Ngoc, J. F. Teichert, *Chem. Eur. J.* **2020**, *26*, 1597–1603.
- [92] H. Konnerth, M. H. G. Pechtl, *Chem. Commun.* **2016**, *52*, 9129–9132.
- [93] M. D. de los Bernardos, S. Pérez-Rodríguez, A. Gual, C. Claver, C. Godard, *Chem. Commun.* **2017**, *53*, 7894–7897.
- [94] K. Murugesan, A. S. Alshammari, M. Sohail, M. Beller, R. V. Jagadeesh, *J. Catal.* **2019**, *370*, 372–377.
- [95] A. Valiente, P. Martínez-Pardo, G. Kaur, M. Johansson, B. Martín-Matute, *ChemSusChem* **2022**, *15*, e202102221.
- [96] M.-Y. Lee, C. Kahl, N. Kaeffer, W. Leitner, *JACS Au* **2022**, *2*, 573–578.
- [97] Y. Chai, G. Wu, X. Liu, Y. Ren, W. Dai, C. Wang, Z. Xie, N. Guan, L. Li, *J. Am. Chem. Soc.* **2019**, *141*, 9920–9927.
- [98] X. Shi, X. Wen, S. Nie, J. Dong, J. Li, Y. Shi, H. Zhang, G. Bai, *J. Catal.* **2020**, *382*, 22–30.
- [99] B. L. Ramirez, C. C. Lu, *J. Am. Chem. Soc.* **2020**, *142*, 5396–5407.
- [100] R. K. Rai, M. K. Awasthi, V. K. Singh, S. R. Barman, S. Behrens, S. K. Singh, *Catal. Sci. Technol.* **2020**, *10*, 4968–4980.
- [101] For a review on copper-catalyzed hydrogenation reactions, including alkyne semi-hydrogenations, see: L. T. Brechman, J. F. Teichert, *Synthesis* **2020**, *52*, 2483–2496.
- [102] For a perspective on regioselective transformations of alkynes catalyzed by copper hydride or boryl copper species, see: T. Fujihara, K. Semba, J. Terao, Y. Tsuji, *Catal. Sci. Technol.* **2014**, *4*, 1699–1709.
- [103] For alternative stereoselective synthesis by copper-catalyzed hydrosilylation of alkynes, see for example: a) H. Jang, A. R. Zhugralin, Y. Lee, A. H. Hoveyda, *J. Am. Chem. Soc.* **2011**, *133*, 7859–7871; b) H. Yoshida, Y. Takemoto, K. Takaki, *Chem. Commun.* **2014**, *50*, 8299–8302; c) Q.-Q. Xuan, C.-L. Ren, L. Liu, D. Wang, C.-J. Li, *Org. Biomol. Chem.* **2015**, *13*, 5871–5874; d) W. J. Jang, B.-N. Kang, J. H. Lee, Y. M. Choi, C.-H. Kim, J. Yun, *Org. Biomol. Chem.* **2019**, *17*, 5249–5252; e) Z.-L. Wang, F.-L. Zhang, J.-L. Xu, C.-C. Shan, M. Zhao, Y.-H. Xu, *Org. Lett.* **2020**, *22*, 7735–7742; f) X. Lu, W. Ming, A. Friedrich, F. Kerner, T. B. Marder, *Angew. Chem. Int. Ed.* **2020**, *59*, 304–309.
- [104] For alternative stereoselective synthesis by copper-catalyzed hydroboration of alkynes, see for example: a) T. Fujihara, K. Semba, J. Terao, Y. Tsuji, *Catal. Sci. Technol.* **2014**, *4*, 1699–1709; b) W. J. Jang, W. L. Lee, J. H. Moon, J. Y. Lee, J. Yun, *Org. Lett.* **2016**, *18*, 1390–1393; c) J. S. da Costa, R. K. Braun, P. A. Horn, D. S. Lüdtkke, A. V. Moro, *RSC Adv.* **2016**, *6*, 59935–59938; d) Z.-J. Yao, S. Hong, W. Zhang, M. Liu, W. Deng, *Tetrahedron Lett.* **2016**, *57*, 910–913; e) S. Krautwald, M. J. Bezdek, P. J. Chirik, *J. Am. Chem. Soc.* **2017**, *139*, 3868–3875; f) Y. Gao, Z.-Q. Wu, K. M. Engle, *Org. Lett.* **2020**, *22*, 5235–5239.
- [105] K. Semba, R. Kameyama, Y. Nakao, *Synlett* **2015**, *26*, 318–322.
- [106] F. Pape, N. O. Thiel, J. F. Teichert, *Chem. Eur. J.* **2015**, *21*, 15934–15938.
- [107] N. O. Thiel, J. F. Teichert, *Org. Biomol. Chem.* **2016**, *14*, 10660–10666.
- [108] T. Wakamatsu, K. Nagao, H. Ohmiya, M. Sawamura, *Organometallics* **2016**, *35*, 1354–1357.
- [109] a) A. Fedorov, H.-J. Liu, H.-K. Lo, C. Copéret, *J. Am. Chem. Soc.* **2016**, *138*, 16502–16507; b) O. G. Salnikov, H.-J. Liu, A. Fedorov, D. B. Burueva, K. V. Kovtunov, C. Copéret, I. V. Koptuyug, *Chem. Sci.* **2017**, *8*, 2426–2430; c) N. Kaeffer, K. Larmier, A. Fedorov, C. Copéret, *J. Catal.* **2018**, *364*, 437–445.
- [110] N. Kaeffer, H.-J. Liu, H.-K. Lo, A. Fedorov, C. Copéret, *Chem. Sci.* **2018**, *9*, 5366–5371.
- [111] H. Cao, T. Chen, Y. Zhou, D. Han, S.-F. Yin, L.-B. Han, *Adv. Synth. Catal.* **2014**, *356*, 765–769.
- [112] a) K. Semba, T. Fujihara, T. Xu, J. Terao, Y. Tsuji, *Adv. Synth. Catal.* **2012**, *354*, 1542–1550; b) A. M. Whittaker, G. Lalic, *Org. Lett.* **2013**, *15*, 1112–1115; c) N. Cox, H. Dang, A. M. Whittaker, G. Lalic, *Tetrahedron* **2014**, *70*, 4219–4231; d) G.-H. Wang, H.-Y. Bin, M. Sun, S.-W. Chen, J.-H. Liu, C.-M. Zhong, *Tetrahedron* **2014**, *70*, 2175–2179; e) J. W. Hall, D. M. L. Unson, P. Brunel, L. R. Collins, M. K. Cybulski, M. F. Mahon, M. K. Whittlesey, *Organometallics* **2018**, *37*, 3102–3110.
- [113] L. Duan, K. Jiang, H. Zhu, B. Yin, *Org. Biomol. Chem.* **2021**, *19*, 365–369.
- [114] H. Bao, B. Zhou, H. Jin, Y. Liu, *J. Org. Chem.* **2019**, *84*, 3579–3589.
- [115] J. Huang, X. Li, H. Wen, L. Ouyang, N. Luo, J. Liao, R. Luo, *ACS Omega* **2021**, *6*, 11740–11749.
- [116] E. Korytiaková, N. O. Thiel, F. Pape, J. F. Teichert, *Chem. Commun.* **2017**, *53*, 732–735.
- [117] T. Kaicharla, B. M. Zimmermann, M. Oestreich, J. F. Teichert, *Chem. Commun.* **2019**, *55*, 13410–13413.
- [118] M. J. Moran, K. Martina, V. Bieliunas, F. Baricco, S. Tagliapietra, G. Berlier, W. M. De Borggraeve, G. Cravotto, *Adv. Synth. Catal.* **2021**, *363*, 2850–2860.
- [119] B. Y. Park, T. Lim, M. S. Han, *Chem. Commun.* **2021**, *57*, 6891–6894.
- [120] R. Kusy, K. Grela, *Green Chem.* **2021**, *23*, 5494–5502.
- [121] H. Kominami, M. Higa, T. Nojima, T. Ito, K. Nakanishi, K. Hashimoto, K. Imamura, *ChemCatChem* **2016**, *8*, 2019–2022.
- [122] For zinc-catalyzed hydrosilylation of alkynes, see for example: T. Tani, Y. Sohma, T. Tsuchimoto, *Adv. Synth. Catal.* **2020**, *362*, 4098–4108.
- [123] For zinc-catalyzed hydroboration of alkynes, see for example: a) Y. Nagashima, R. Takita, K. Yoshida, K. Hirano, M. Uchiyama, *J. Am. Chem. Soc.* **2013**, *135*, 18730–18733; b) R. J. Procter, M. Uzelac, J. Cid, P. J. Rushworth, M. J. Ingleson, *ACS Catal.* **2019**, *9*, 5760–5771; c) S. Mandal, S. Mandal, K. Geetharani, *Chem. Asian J.* **2019**, *14*, 4553–4556; d) M. Uzelac, K. Yuan, M. J. Ingleson, *Organometallics* **2020**, *39*, 1332–1338.
- [124] R. Maazaoui, R. Abderrahim, F. Chemla, F. Ferreira, A. Perez-Luna, O. Jackowski, *Org. Lett.* **2018**, *20*, 7544–7549.

Manuscript received: July 13, 2022  
Revised manuscript received: August 25, 2022  
Accepted manuscript online: August 26, 2022  
Version of record online: September 15, 2022